CHALMERS TEKNISKA HÖGSKOLA

GEOHYDROLOGISKA FORSKNINGSGRUPPEN

Institutionerna för:

Geologi

Geoteknik med grundläggning

Vattenbyggnad

Vattenförsörjnings- och avloppsteknik

INTERIM REPORT

MATHEMATICAL MODELS FOR GRADUALLY VARIED UNSTEADY FREE SURFACE FLOW

Development and Discussion of Basic Equations.
Preliminary Studies of Methods for Flood Routing in Storm Drains.

ANDERS SJÖBERG

Meddelande nr 8

GÖTEBORG 1974

This interimreport is submitted in partially fulfillment of project No 730276-7: Storm-Water Runoff- Flow Models for Sewer Systems, under the sponsorship of the Swedish Council for Building Research.

CONTENTS

1. INTRODUCTION

1.1 Objectives of the investigation

In recent years there has been an increasing interest in urban runoff problems. The pollutants carried by storm water runoff are, with present views on pollution problems, no longer negligible. Further more, in combined sewer systems, untreated domestic waste water is diverted during storm periods. This inconvenience may be avoided by converting the combined system into separate sewer systems. However, the large investments connected with such solution makes it natural to look at less expensive methods which also can improve the pollution situation. For example, overflow reduction may be obtained by furnishing combined systems with storage tanks. This technique may under certain conditions represent a less expensive alternative to a change from combined to a separate sewer system. However, the analysis and optimization of combined networks, as well as design of storm drain systems, must be based on mathematical models [1, 2, 3, 4].

The fast development of digital computer technique enhances the feasibility of mathematical modelling of urban runoff. Most of the designed models are deterministic, that is, the model is designed so that when a problem is stated, its solution leads to an exact prediction of what will happen (in contrast to a stochastic model, in which a statement of a problem leads to a prediction of events occurring with certain probabilities). Examples of such deterministic models are the NIVA-sewer network model [2], the EPA-storm water management model [3], Dorsch Consult - hydrograph volume method [4, 5], the RRL-method for urban runoff [7, 8, 11], and the models presented in [6, 9, 10 46]. All these models include in a more or less approximative way every hydrological component needed to describe a runoff situation (precipitation, surface storage, infiltration, surface runoff, channel and conduit routing, storage routing). However, we are here concerned with channel and pipe routing procedures only, that is, description of storm water runoff in sewer networks.

As indicated by the title, the present study of unsteady free surface flow in storm drains has the primary objective to compare the accuracy of various methods for flood routing. To the authors knowledge no such investigation has yet been reported. The methods to be compared are, taken from the most simplified to the most detailed one from hydrodynamical point of view,

- the flood wave (the routed rain water hydrograph) considered as a kinematic wave [6, 9]
- the RRL approach [7, 8, 11]
- the NIVA model (a modification of the RRL approach) [1, 2]
- the EPA model (routing considering actual flow velocities) [3]
- numerical solution of the complete onedimensional equations governing unsteady free-surface flow, [12] and probably [5]

"Rational" type methods, which neglect the reservoir retention in the storm drains, are not considered. Unit hydrograph methods are also disregarded [16, 43].

Comparison of the solution of the complete one-dimensional equations by numerical methods with observed routed hydrographs show good agreement [12, 13, 14, 15]. These solutions may thus be taken as basis for judging the accuracy of the other methods. Even for large experimental facilities, the observational errors on flood waves, produced in pipes and channels, are large. It is therefore very difficult to distinguish computional errors in the numerical solution from errors in boundary and initial conditions and in basic assumptions underlying the governing equations, on the basis of differences between observed and computed waves.

1.2 Problem to be studied

The properties of a routing storm water wave (hydrograph) are functions of channel geometry, boundary and initial conditions. Even for chematized conditions a great number of parameters are required for the description of the propagation of a wave. It is thus suggested, that comparative studies are limited to the comparison of the accuracy of flood routing procedures in the case of a pipe of constant bottom slope and circular section. The inflow hydrograph is assumed to be composed of a symmetrical triangular time-discharge relation overlying a constant base flow, see fig. 3.1, page 3.

We consider here only partly filled pipe sections and subcritical conditions. Problems concerning sewer systems flowing partly full and simulation of backwater conditions will be dealt with in a coming investigation.

In chapter 2 the two basic equations - the equation of continuity and the equation of motion - governing incompressible gradually varied unsteady free surface flow are derived. The properties of these two equations are analyzed in chapter 3, where also possible wave types (dynamic waves, kinematic waves, etc) and their properties are discussed.

In chapter 4, various flood routing models (i. e. more or less approximative numerical solutions of the basic equations) are presented and analyzed. Finally, in chapter 5, the models are tested against each other for one specific flow case. More extensive comparisons will be made when computer programs are available.

2. BASIC EQUATIONS FOR GRADUALLY VARIED UNSTEADY FREE SURFACE FLOW

This chapter is concerned with the development of the two basic equations governing incompressible gradually varied unsteady free surface flow in conduits or channels:

- the equation of continuity based on the principle of conservation of mass
- the equation of motion derived from Newton´s second law

For gradually varied flow it is assumed that the streamline curvatures are small and that the velocity components normal to the direction of motion are negligible compared to longitudinal velocities. If the flow is in the x-direction, the pressure distribution in the yz-plane may then be assumed to be hydrostatic. This assumption leads to a one-dimensional analysis of the fluid motion.

The one-dimensional equations (generally called the Saint-Venant equations) are derived by integrating the general equations of continuity and motion over the cross section of flow. The integration is performed under the following idealized conditions:

- the slope of the bottom channel is small
- the velocity is parallel to the bottom
- the velocity distribution is uniform over each cross section
- water is a homogeneous incompressible fluid
- the channel section is stable

In free surface flow, water is satisfactorily treated as an incompressible fluid, the pressure range involved being small.

In most cases water may also be treated as a uniform-density fluid. This assumption is valid unless there exists a pronounced density stratification within the fluid. An example of such a non-negligible density stratification in free-surface channel flow is the interfacial layer between fresh water and sea-water in river mouths and estuaries.

In the present flow case, storm water runoff in pipes and tunnels, pronounced vertical density stratifications can be obtained by non-uniform distributions of suspended material in storm water. However, information concerning the concentration of suspended material in storm water runoff in urban areas indicates that flow in storm-sewers may be analyzed as a density homogeneous flow with sufficient accuracy.

The equations of continuity and of motion thus derived are, in the case of no lateral inflow, given by eq. (2.1.10) and eq. (2.2.18), respectively

$$\frac{\partial Q}{\partial x} + \frac{\partial A}{\partial t} = 0;$$

$$\frac{1}{g}\frac{\partial}{\partial t}\left(\frac{Q}{A}\right) + \frac{\partial}{\partial x}\left(\frac{Q^2}{2gA^2}\right) + \frac{\partial Y}{\partial x} = S_o - S_f;$$

where

A = channel cross-sectional area
Q = discharge
Y = water depth
S_o = channel bottom slope
S_f = friction slope
x = distance in the direction of flow
t = time
g = acceleration of gravity

2.1 Equation of continuity

The equation of continuity is based on the principle of conservation of mass. It follows from this principle that the net flux of mass into the differential control volume in fig. 2.1 must equal the time rate of change of mass within the volume. Thus, as Δx, Δy, $\Delta z \rightarrow 0$, [17]

$$\frac{\partial \rho}{\partial t} + \nabla \cdot (\rho \vec{v}) = 0; \qquad (2.1.1\ a)$$

or in an alternative form

$$\frac{d\rho}{dt} + \rho\, \nabla \cdot \vec{v} = 0; \qquad (2.1.1\ b)$$

where

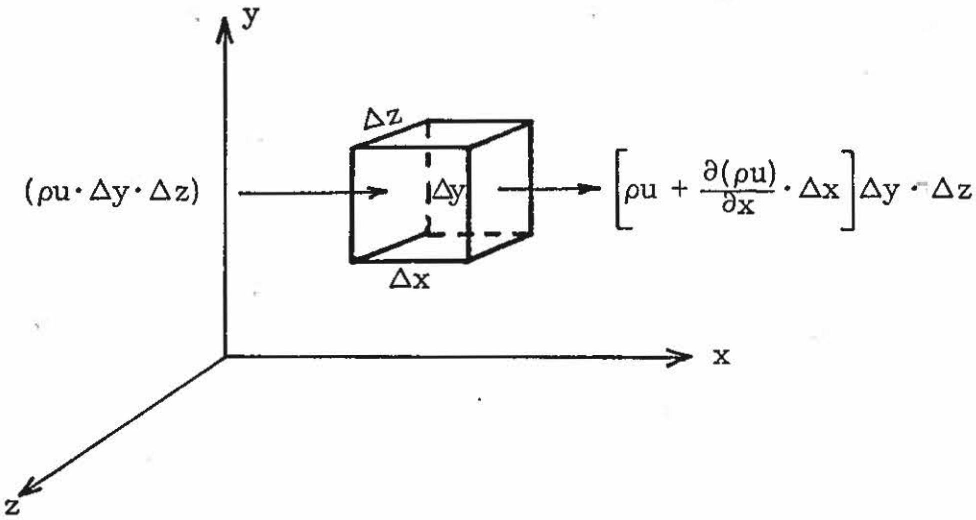

Fig. 2.1 Differential control volume for conservation of mass

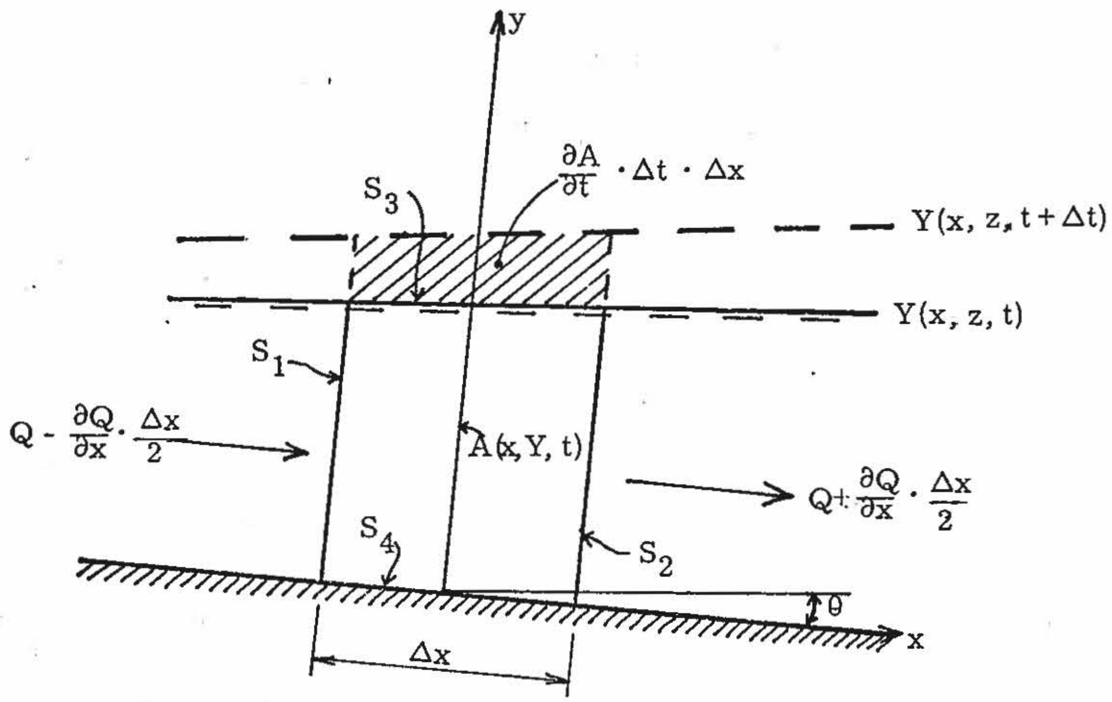

Fig. 2.2 Variable differential control volume

ρ = density of fluid
t = time
$\vec{v}$ = velocity vector $(u, v, w)^x$
u, v, w = Cartesian velocity components
∇ = vector differential operator $(\partial/\partial x; \partial/\partial y; \partial/\partial z)^x$
$\nabla \cdot \rho\vec{v}$ = $\rho \; \nabla \cdot \vec{v} + \vec{v} \cdot \nabla \rho$
$\nabla \cdot \vec{v}$ = $\partial u/\partial x + \partial v/\partial y + \partial w/\partial z$
$\nabla \rho$ = $(\partial \rho/\partial x, \; \partial \rho/\partial y, \; \partial \rho/\partial z)^x$
$\vec{v} \cdot \nabla \rho$ = $u \, \partial \rho/\partial x + v \, \partial \rho/\partial y + w \, \partial \rho/\partial z$

Integration of eq. (2.1.1 a) over a variable volume of space W, completely filled with fluid, gives

$$\int_W \left[\frac{\partial \rho}{\partial t} + \nabla \cdot (\rho\vec{v})\right] dW = 0; \qquad (2.1.2)$$

The second term is transformed from a volume integral to a surface integral by the divergence theorem, which states [18, 19, 20]

$$\int_W \nabla \cdot \vec{G} \, dW = \int_S \vec{G} \cdot \vec{n} \, dS \qquad (2.1.3)$$

where $\vec{G}$ = a continuous vector with continuous partial derivatives, S = the bounding surface and n = $(n_x, n_y, n_z)^x$ = outward unit vector normal to dS. Thus eq. (2.1.2) becomes

$$\int_W \left(\frac{\partial \rho}{\partial t}\right) dW + \int_S \rho\vec{v} \cdot \vec{n} \, dS = 0; \qquad (2.1.4)$$

After applying the general transport theorem [18, 21]

$$\frac{d}{dt} \int f \, dW = \int \frac{\partial f}{\partial t} \, dW + \int f \, (\vec{w} \cdot \vec{n}) \, dS; \qquad (2.1.5)$$

in which f = a continuous scalar or vector function and $\vec{w}$ = the local velocity at the surface, the left hand side of eq. (2.1.4) turns into

$$\frac{d}{dt}\int_W \rho\, dW + \int_S \rho\, (\vec{v} - \vec{w}) \cdot \vec{n}\, dS = 0; \tag{2.1.6}$$

For a homogeneous incompressible flow the density is independant of both time and space. Hence it follows from eq. (2.1.6) that

$$\frac{dW}{dt} + \int_S (\vec{v} - \vec{w}) \cdot \vec{n}\, dS = 0; \tag{2.1.7}$$

This equation will now be applied to the variable control volume in fig. 2.2.

The open-channel flow in fig. 2.2 is defined by the waterdepth $Y = Y(x, z, t)$ normal to the channel bottom, the cross-sectional area of flow $A = A(x, Y, t)$ in the yz-plane and the discharge $Q = Q(x, t)$. A slice of thickness Δx and area A at its midsection is chosen as differential control volume to which eq. (2.1.7) will now be applied. Analysing the equation term by term we obtain

the first term: because the x-coordinate is kept constant

$$\frac{dW}{dt} = \frac{\partial W}{\partial t} = \frac{\partial A}{\partial t} \cdot \Delta x; \tag{2.1.8}$$

the second term:

$$\int_S (\vec{v}-\vec{w}) \cdot \vec{n}\, dS = \int_{S_2} \vec{v} \cdot \vec{n}\, dS + \int_{S_1} \vec{v} \cdot \vec{n}\, dS = \frac{\partial}{\partial x} \int_A \vec{v} \cdot \vec{n}\, dS = \tag{2.1.9}$$

$$= \frac{\partial Q}{\partial x} \cdot \Delta x;$$

which leads to the equation of continuity for uniform density, incompressible free-surface flow in case of no lateral inflow

$$\frac{\partial Q}{\partial x} + \frac{\partial A}{\partial t} = 0; \tag{2.1.10}$$

which may be derived also from eq. (2.1.1b), which in case of an incompressible fluid takes the form [17], $d\rho/dt = \rho\, \nabla \cdot \vec{v} = 0$.

Considering a prismatic channel, the cross-sectional area A can be expressed as a unique function of Y (if the free-surface is horizontal in the yz-plane)

$$A = \int_0^Y b(y)\,dy = A(Y); \qquad (2.1.11)$$

where b(y) is the width of the section at level y above the channel bottom, fig. 2.3. Thus

$$\frac{\partial A}{\partial t} = \frac{\partial A}{\partial Y}\cdot\frac{\partial Y}{\partial t} = B\frac{\partial Y}{\partial t}; \qquad \frac{\partial A}{\partial x} = B\frac{\partial Y}{\partial x}; \qquad (2.1.12)$$

where B = top width of flow, V = average velocity.

The equation of continuity may then be written in the alternative forms

$$\frac{\partial Q}{\partial x} + \frac{\partial A}{\partial t} = 0; \qquad (2.1.13a)$$

$$\frac{\partial Q}{\partial x} + B\frac{\partial Y}{\partial t} = 0; \qquad (2.1.13b)$$

$$A\frac{\partial V}{\partial x} + VB\frac{\partial Y}{\partial x} + B\frac{\partial Y}{\partial t} = 0; \qquad (2.1.13c)$$

In case of lateral inflow q per unit channel length Δx, (2.1.13a) takes the form

$$\frac{\partial Q}{\partial x} + \frac{\partial A}{\partial t} = q; \qquad (2.1.14)$$

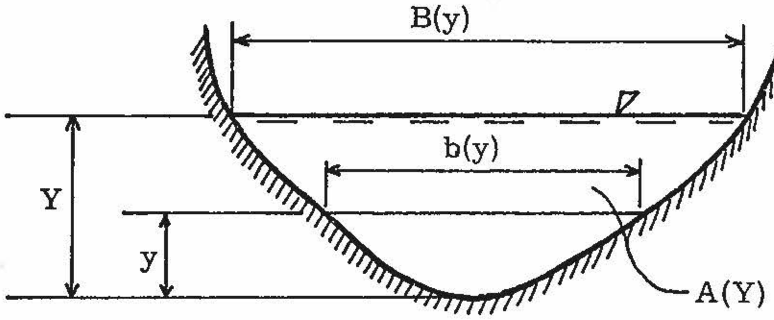

Fig. 2.3 Geometric elements of a cross-sectional area of flow.

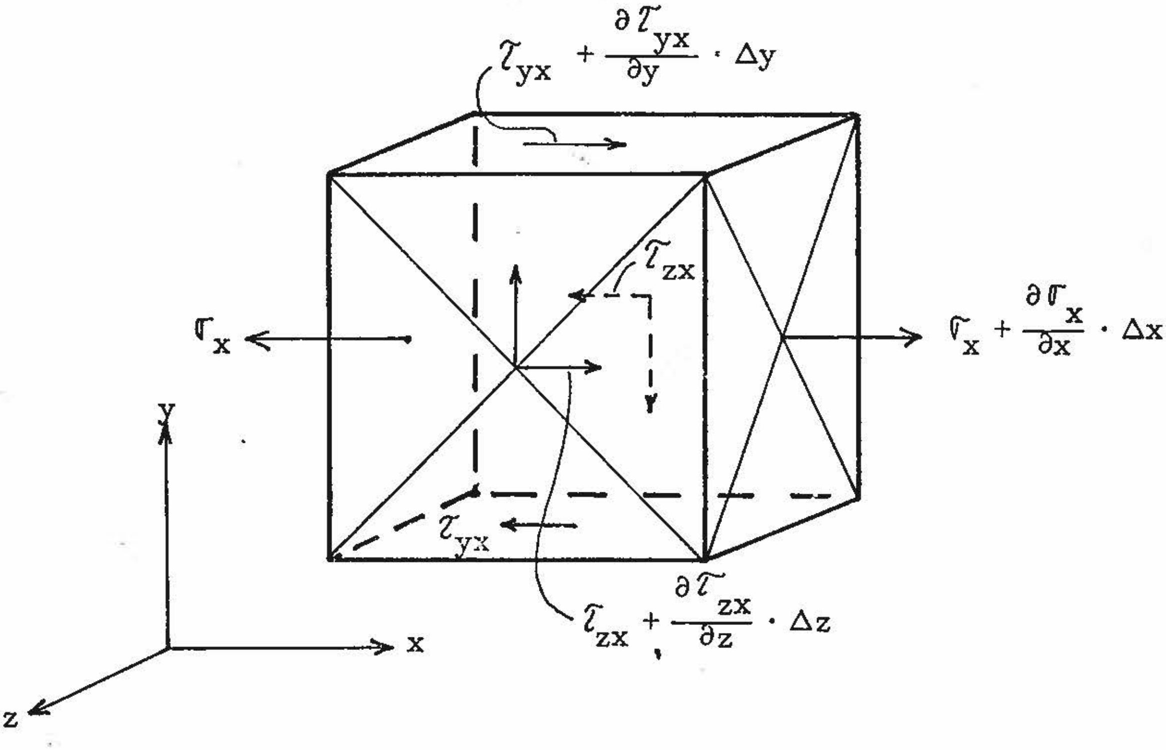

Fig. 2.4 Tangential and normal stresses in the x-direction on a differential control volume $\Delta x\ \Delta y\ \Delta z$.

2.2 The equation of motion

The equation of motion is derived from Newton's second law, which states that the vector sum $\vec{F}$ of all forces acting on a mass element equals the time rate of change of the momentum vector

$$\vec{F} = \frac{d}{dt}(\Delta m \cdot \vec{v});$$

where Δm is the mass of a fluid element. This leads to the equation of motion (the momentum equation), which component in the x-direction is [17, 19]

$$\frac{\partial u}{\partial t} + \vec{v} \cdot \nabla u = g_x - \frac{1}{\rho}\frac{\partial p}{\partial x} + \frac{1}{\rho}\left(\frac{\partial \sigma_x'}{\partial x} + \frac{\partial \tau_{yx}}{\partial y} + \frac{\partial \tau_{zx}}{\partial z}\right); \qquad (2.2.1)$$

where

u = x-component of velocity

g_x = x-component of acceleration of gravity

p = pressure

σ_x' = deviation of the normal stress $-\sigma_x$ from the pressure p; ($\sigma_x = -p + \sigma_x'$)

τ_{yx}, τ_{zx} = tangential stresses defined in fig. 2.4

The equation is assumed to be averaged over a long time in comparison to the actual time scale of turbulence.

Integration with respect to an arbitrary control volume filled with fluid gives for a uniform density, incompressible fluid

$$\int_W \left[\frac{\partial u}{\partial t} + \nabla \cdot u\vec{v} - g_x + \frac{1}{\rho}\left(\frac{\partial p}{\partial x} - \frac{\partial \sigma_x'}{\partial x} - \frac{\partial \tau_{yx}}{\partial y} - \frac{\partial \tau_{zx}}{\partial z}\right)\right] dW = 0; \qquad (2.2.2)$$

noting that $\vec{v} \cdot \nabla u = \nabla \cdot u\vec{v} - u\nabla \cdot \vec{v} = \nabla \cdot u\vec{v}$ by virtue of the continuity equation for incompressible fluids, $d\rho/dt = \rho u\ \nabla \cdot \vec{v} = 0$. Application of the general transport theorem, eq. (2.1.5), to the first term and the divergence theorem, eq. (2.1.3), to the second and the fourth term gives

$$\frac{d}{dt}\int_W u\,dW + \int_S u(\vec{v}-\vec{w})\cdot\vec{n}\,dS - \int_W g_x\,dW +$$

$$+\frac{1}{\rho}\int_S (pn_x - \tau'_x n_x)\,dS - \frac{1}{\rho}\int_S (\tau_{yx} n_y + \tau_{zx} n_z)\,dS = 0; \qquad (2.2.3)$$

This equation will now be applied to the variable control volume in fig. 2.2 taking the x-axis as the longitudinal axis of the channel parallel to the channel bottom. Analyzing eq. (2.2.3) term by term, we obtain:

the first term:

Because the x-coordinate is kept constant we may write

$$\frac{d}{dt}\int_W u\,dW = \frac{\partial}{\partial t}\int_W u\,dW = \frac{\partial Q}{\partial t}\Delta x; \qquad (2.2.4)$$

the second term:

$$\int_S u(\vec{v}-\vec{w})\cdot\vec{n}\,dS = \int_{S_2} u^2 dS - \int_{S_1} u^2 dS = \frac{\partial}{\partial x}\int_A u^2 dS\Delta x =$$

$$= \frac{\partial}{\partial x}\left(\beta\frac{Q^2}{A}\right)\Delta x; \qquad (2.2.5)$$

with

$$\beta = \frac{A}{Q^2}\int_A u^2 dS;$$

where β = 1 if the velocity distribution is uniform over each cross-section.

the third term:

$$-\int_W g_x\,dW = -gA\,dx\cdot\sin\theta = -gA\,S_o\Delta x;$$

where θ = angle inclination of the channel bottom, g = acceleration of gravity and S_o = channel bottom slope.

<u>the fourth term:</u>

The pressure p = p (x, y, z, t) is composed of a hydrostatic portion, due to submergence of the point below the free surface, and dynamic components related to streamline curvature, spatial variation in turbulence parameters, etc. and may be obtained by integrating the y- and z-components of the equations of motion, which considers the pattern of the mean turbulente motion. Reynolds converted the equations of motion for an incompressible fluid into a form which does that [17]. These equations may be written:

$$\frac{\partial p}{\partial y} = F_{yp} + F_{yt} + \rho g_y;$$

$$\frac{\partial p}{\partial z} = F_{zp} + F_{zt} + \rho g_z; \qquad (2.2.6)$$

where

$$F_{yp} = - \rho \left(\frac{\partial v}{\partial t} + u \frac{\partial v}{\partial x} + v \frac{\partial v}{\partial y} + w \frac{\partial v}{\partial z}\right) + \mu \nabla^2 v;$$

$$F_{yt} = - \rho \left(\frac{\partial \overline{u'v'}}{\partial x} + \frac{\partial \overline{v'v'}}{\partial y} + \frac{\partial \overline{v'w'}}{\partial z}\right);$$

$$F_{zp} = - \rho \left(\frac{\partial w}{\partial t} + u \frac{\partial w}{\partial x} + v \frac{\partial w}{\partial y} + w \frac{\partial w}{\partial z}\right) + \mu \nabla^2 w;$$

$$F_{zt} = - \rho \left(\frac{\partial \overline{u'w'}}{\partial x} + \frac{\partial \overline{v'w'}}{\partial y} + \frac{\partial \overline{w'w'}}{\partial z}\right);$$

$$g_y = - g \cos \theta; \qquad g_z = 0;$$

$$u = \frac{1}{T} \int_0^T u(t)\, dt$$ etc for p, v, w with T being a long time in comparison with the time scale of turbulence

$u' = u(t) - u$ = turbulent fluctuating component of u; etc. for v, w.

$$\overline{u'} = \frac{1}{T} \int_0^T u' dt = 0;$$

$\overline{u'w'}$ = time mean value of $(u'w')$

$$\nabla^2 v = \frac{\partial^2 v}{\partial x^2} + \frac{\partial^2 v}{\partial y^2} + \frac{\partial^2 v}{\partial z^2};$$

$\mu = \nu / \rho$ = dynamic viscosity of the fluid.

Integration in the yz-plane with respect to y and z, respectively, gives (see also fig. 2.5)

$$p(x, Y, z, t) - p(x, y, z, t) = \int_{y}^{Y} (F_{yp} + F_{yt})\, dy - \rho g\, (Y-y) \cos\theta\,;$$

$$p\,(x, Y, z, t) - p(x, Y, 0, t) = \int_{0}^{z} (F_{zp} + F_{zt})\, dz; \qquad (2.2.7)$$

and we finally obtain

$$p = p\,(x, y, z, t) = \rho g\, (Y - y) \cos\theta + C_t + C_p; \qquad (2.2.8)$$

where, [22]

$$C_t = - \int_{y}^{Y} F_{yt}\, dy + \int_{0}^{z} F_{zt}\, dz; \qquad \text{(turbulence correction)}$$

$$C_p = - \int_{y}^{Y} F_{yp}\, dy + \int_{0}^{z} F_{zp}\, dz; \qquad \text{(correction for nonuniformity and unsteadiness)}$$

$$p(x, Y, 0, t) = \text{atmospheric pressure} = 0;$$

The second part of the fourth term σ_x' is by definition [17]

$$\sigma_x' = 2\mu \frac{\partial u}{\partial x} - \rho \overline{u'u'}; \qquad (2.2.9)$$

To be able to integrate the fourth term over a cross section of flow in a useful form, we have to assume $C_t + C_p - \sigma_x' = 0$. The underlying assumptions follow from the discussion below.

For gradually varied flow it is generally assumed that the streamline curvatures are small and that the velocity components normal to the direction of flow, in this case the x-axis, are negligible. Thus all terms in eq. (2.28) and eq. (2.2.9) which are functions of v and w are disregarded. Moreover, assuming turbulent flow, viscous stresses ($\mu\partial v/\partial x$; $\mu\partial v/\partial y$; etc.) are much

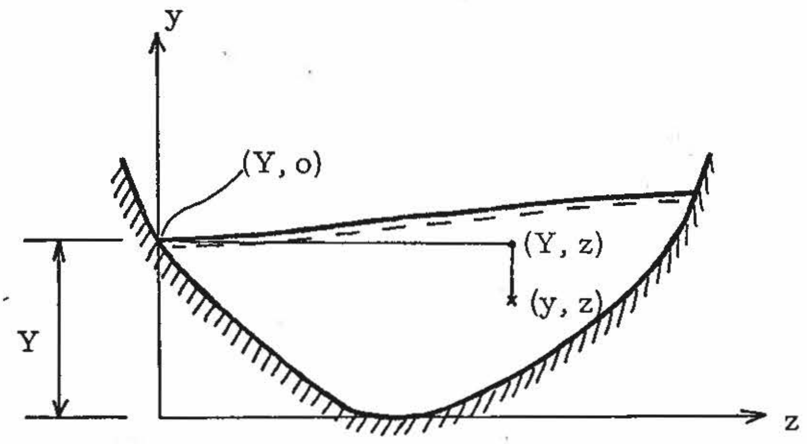

Fig. 2.5 Sketch of definition

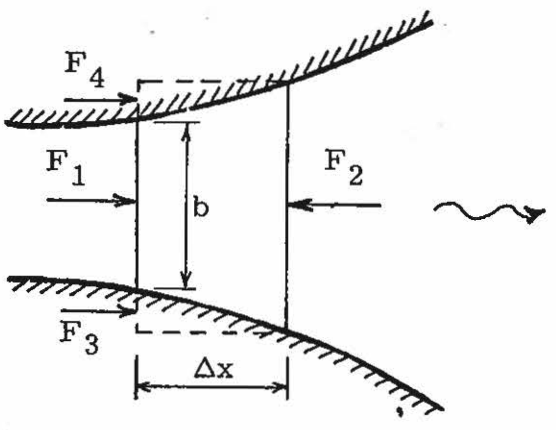

Fig. 2.6 Hydrostatic forces in the x-direction

smaller than the Reynolds stresse ($\rho\overline{u'v'}$; $\rho\overline{v'w'}$; $\rho\overline{u'w'}$) and may also be neglected. The correction term C_p for nonuniformity and unsteadiness may thus be assumed zero.

As regards C_t, we may assume that the turbulent shear stresses are only weak functions of x. Cancelling the derivatives with respect to x we then have

$$C_t\,(x,y,z,t) = \int_y^Y \rho\,\left(\frac{\partial \overline{v'v'}}{\partial y}\right) dy - \int_0^z \rho\,\left(\frac{\partial \overline{w'w'}}{\partial z}\right) dz = \qquad (2.2.9)$$

$$= -\rho\overline{v'v'} - \rho\overline{w'w'};$$

if we assume that $\rho\overline{v'v'}$ vanishes at the free surface and that $\rho\overline{w'w'}$ equals zero at the wall.

Moreover, measurements indicate [23, 24, 25], that $\rho\overline{v'v'} \approx \rho\overline{w'w'}$ and $\rho\overline{u'u'} \approx 2\,\rho\overline{v'v'}$, from which it follows that

$$C_t \approx -2\,\rho\overline{v'v'} \approx -\rho\overline{u'u'}; \qquad (2.2.10)$$

Now, the second part of the fourth term is by definition, assuming turbulent flow,

$$\sigma_x' = -\rho\overline{u'u'} = C_t; \qquad (2.2.11)$$

Thus, with $C_p = 0$ we have

$$p - \sigma_x' = -\sigma_x = \rho g\,(Y - y)\cos\theta; \qquad (2.2.12)$$

which indicates that for gradually varied flow, the normal stress distribution in planes perpendicular to the flow direction is approximately hydrostatic. However, as σ_x' is small, this statement also holds for the pressure distribution. Thus

$$p \approx \rho g\,(Y - y)\cos\theta; \qquad (2.2.13)$$

We also note from eq. (2.2.13) that $\partial p/\partial z = 0$, which implies that the water surface is horizontal. For this condition the fourth term becomes (see fig. 2.6)

$$\frac{1}{\rho}\int_S (p - \sigma_x') n_x \, dS = \int_S g(Y - y) \cos\theta \cdot n_x \, dS =$$

$$= (F_2 - F_1) - (F_3 + F_4) = \frac{\partial}{\partial x}\int_0^Y g(Y - y) \, b \cos\theta \cdot dy \, \Delta x - \quad (2.2.14)$$

$$- \int_0^Y g(Y - y) \frac{\partial b}{\partial x} \cos\theta \cdot dy \, \Delta x = g A \frac{\partial Y}{\partial x} \cdot \Delta x \cdot \cos\theta;$$

As it is seen from eq. (2.2.14), the influence of a nonhydrostatic pressure distribution on the one-dimensional equations of motion is felt from section to section only through the variation in σ_x', C_p, C_t. However, as pointed out in [12], there has apparently been no attempt to quantify the effects of the above assumptions on computed waves along the flow channel. The term "gradually varied flow" may then be subjected to different interpretations by various investigators.

For gradually varied flow, as rainfall runoff in storm drains, the effect of the above assumptions are so small, that they are practically impossible to investigate even for controlled laboratory conditions with a conduit or channel, the experimental error being too large.

The fifth term:

The fifth term is expressed as

$$\frac{1}{\rho}\int_S (\tau_{yx} n_y + \tau_{zx} n_z) dS = - \frac{\tau_o}{\rho} \cdot P \Delta x; \quad (2.2.15)$$

where τ_o = mean wall shear stress and P = wetted perimeter.

τ_o has to be determined from empirical or semi-empirical relations such as the Chezy and the Manning formulas and the Darcy equation [17]. In these formulas, established for uniform flow, τ_o is expressed as a function of local velocity, geometric conditions and a friction factor, which in its turn is a function of Reynolds number, geometric conditions and wall roughness.

For lack of sufficient information it is customary to assume that in gradually varied flow the friction factors defined for uniform flow are not affected by the unsteadiness and nonuniformity of the flow.

Summation of the five terms finally gives the one-dimensional form of the equation of motion.

$$\frac{\partial Q}{\partial t} + \frac{\partial}{\partial x}\left(\beta \frac{Q^2}{A}\right) + gA\frac{\partial Y}{\partial x}\cos\theta = gAS_o - \frac{\tau_o P}{\rho}; \qquad (2.2.16)$$

which may also be written

$$\frac{1}{g}\frac{\partial}{\partial t}\left(\frac{Q}{A}\right) + \frac{\partial}{\partial x}\left(\frac{\beta Q^2}{2gA^2}\right) + \frac{\partial Y}{\partial x}\cos\theta = S_o - S_f - \frac{1}{g}\left[\frac{Q^2}{2A^2}\cdot\frac{\partial\beta}{\partial x} + (\beta - 1)\frac{Q}{A^2}\cdot\frac{\partial Q}{\partial x}\right]; \qquad (2.2.17)$$

where

$$S_f = \tau_o P/\rho g A = \text{friction slope}$$

The velocity coefficient β has for turbulent uniform flow a value very close to 1.0. Data presented in [26] indicate, that for pipe flow, β has a value of approximately 1.01 at water depths greater than half the pipe diameter. The data also show a very slight increase in β as depth decreases.

Usually, β is assumed constant and equal to 1.0. Moreover, the channel slope is normally small, why $\cos\theta \approx 1$. Eq. (2.2.17) then becomes

$$\frac{1}{g}\cdot\frac{\partial}{\partial t}\left(\frac{Q}{A}\right) + \frac{1}{2g}\cdot\frac{\partial}{\partial x}\left(\frac{Q}{A}\right)^2 + \frac{\partial Y}{\partial x} = S_o - S_f; \qquad (2.2.18)$$

which is the most frequently used form of the one-dimensional equation of gradually varied, unsteady free surface flow with no lateral inflow.

In the case of a lateral inflow $q > 0$ per unit channel length the quantity $(-qu_1)$, where u_1 = the x-component of the inflow-velocity vector, must be added to eq. (2.2.5). Accounting for the corresponding continuity equation, eq. (2.1.14), the term

$$\frac{q}{gA}\left(u_1 - \frac{Q}{A}\right); \qquad (2.2.19)$$

has to be added on the right hand side of eq. (2.2.18). For lateral outflow, $q < 0$, of zero-velocity components (seepage outflow) the correction term is $(-qQ/gA^2)$.

3. PROPERTIES OF THE BASIC EQUATIONS. DYNAMIC AND KINEMATIC WAVES

3.1 Nondimensional representation of the basic equation

In case of no lateral inflow the one-dimensional form of the equations, (the continuity equation (2.1.10) and the equation of motion (2.2.18)), may be written

$$\frac{\partial Q}{\partial x} + \frac{\partial A}{\partial t} = 0;$$

$$\frac{1}{g}\frac{\partial}{\partial t}\left(\frac{Q}{A}\right) + \frac{1}{2g}\cdot\frac{\partial}{\partial x}\left(\frac{Q}{A}\right)^2 + \frac{\partial Y}{\partial x} = S_o - S_f; \qquad (3.1.1)$$

where

- Q - discharge
- Y = water depth
- A = area of flow (unique function of Y)
- x = distance in the direction of flow
- t = time
- g = acceleration of gravity
- S_o = channel bottom slope
- S_f = friction slope
- Q/A = cross sectional average velocity V

These equations, which are usually named the Saint-Venant equation after A J C Barré de Saint-Venant [19], form a pair of quasi-linear hyperbolic (The significance of this definition appears from section 3.2) partial differential equations in terms of two independant variables x and t, and two dependant variables Q and Y. As dependant variables may also be used Q and A, V and A or V and Y.

Unfortunately, solutions of these equations must be obtained by numerical procedures. Analytical solutions have been obtained only for restricted simplified cases.

A complete formulation of the problem requires definition of boundary and initial conditions. Thus geometric conditions, inflow hydrograph, etc. have to be defined by their characteristic quantities as conduit diameter, peak discharge, etc. Due to the very large number of characteristic quantities necessary to describe generally formulated boundary conditions, an investigation has to be restricted to schematized conditions, for example to those shown in fig. 3.1:

Geometric conditions:

Circular conduit of constant
- diameter D
- wall roughness k
- bottom slope S_o

Boundary conditions:

Symmetric triangular inflow hydrograph defined by
- constant base flow Q_b
- peak flow Q_p
- hydrograph duration t_b

Initial conditions:

Steady discharge equal to the base flow Q_b of the inflow hydrograph.

For the discussion of properties of the equations and for the graphical representation of computed results, it is often advantageous to write equations and boundary conditions in non-dimensional form. This can be done by introducing normalizing quantities. Let

$$Q_o = Q\,(D.\ S_o,\ k,\ \nu\ ) \qquad (3.1.2)$$

be the capacity of the conduit flowing full. ν = the kinematic viscosity of the fluid. Using the Darcy-Wiesbach equation 17

$$S_f = \frac{f}{4R} \cdot \frac{V^2}{2g} = \frac{f}{4R} \cdot \frac{Q^2}{2gA^2}\ ; \qquad (3.1.3)$$

where R = the hydraulic radius A/P and f = friction coefficient being a function of Reynolds number $Re = VR/\nu$ and the relative roughness k/R. Q_o is then defined by the relation $S_f = S_o$ and we obtain

$$Q_o = \frac{\pi D^2}{4} \left(\frac{2g\, S_o\, D}{f_o} \right)^{1/2} \qquad (3.1.4)$$

where

f_o = friction coefficient being a function of the Reynolds number $Re_o = V_o D/$ and the relative roughness k/D.

V_o = the average velocity $4\, Q_o/\pi D^2$

Using these normalizing quantities (Q_o, D, f_o) the following dimensionless variables can be defined

$$Q_x = Q/Q_o; \quad A_x = 4A/\pi D^2; \quad Y_x = Y/D;$$

$$x_x = x/D; \quad t_x = t\, V_o/D; \quad R_x = R/D; \qquad (3.1.5)$$

$$f_x = f/f_o;$$

where V_o = the average velocity $4\, Q_o/\pi D^2$.

If these dimensionless variables are substituted into eq. (3.1.1) the result is

$$\frac{\partial Q_x}{\partial x_x} + \frac{\partial A_x}{\partial t_x} = 0;$$

$$\frac{\partial}{\partial t_x} \left(\frac{Q_x}{A_x} \right) + \frac{1}{2} \frac{\partial}{\partial x_x} \left(\frac{Q_x^2}{A_x^2} \right) + \left(\frac{1}{F_o} \right)^2 \cdot \frac{\partial Y_x}{\partial x_x} = \qquad (3.1.6)$$

$$= \frac{S_o}{F_o^2} (1 - S_{fx})$$

where

F_o = the Froude number $V_o/\sqrt{gD}$

$$S_{fx} = \frac{f_x\, Q_x^2}{4\, R_x A_x^2}$$

The boundary and initial conditions expressed in the same normalizing quantities give

$$Q_x\,(x_x = 0) = Q_x\,(\frac{Q_b}{Q_o};\ \frac{Q_p}{Q_o};\ \frac{t_b V_o}{D};\ t_x);$$

$$f_x = f_x\,(k/D;\ Re_o;\ Q_x\ Y_x); \qquad (3.1.7)$$

It follows from the above equations that a description of the outflow hydrograph in the section $x_x = x/D$ requires seven dimensionless parameters, even for the schematized conditions shown in fig. 3.1. The dependant variables $Q_x\,(x_x,\ t_x)$ and $Y_x\,(x_x,\ t_x)$ defining the outflow hydrograph are thus functions of the parameters

$$F_o,\ S_o;\ (Q_p/Q_o);\ (Q_p/Q_o);\ t_b V_o/D;\ k/D;\ Re_o; \qquad (3.1.8)$$

As no general analytical solution exists, a general picture of the outflow hydrograph can only be found by a systematic variation of the parameters involved (within the range of variation of each parameter) in the computional or the experimental investigations.

It is evident that a graphical or analytical representation of the effects of all these parameters would be rather complicated even if some of the parameters are less important. This stresses the need for further simplification of the boundary conditions, leading to a reduced number of governing parameters. Hence, the following inflow hydrograhp is suggested,

$$Q_x\,(x_x = 0) = Q_x\,(\alpha;\ \gamma;\ \frac{t_b V_o}{D};\ t_x); \qquad (3.1.9)$$

where

$$\alpha = Q_b/Q_o = 0,05;$$
$$\gamma = Q_p/Q_o = 0,95;$$

This simplification, implies a study of the effects of one special type of hydrographs, the limitation justified from practical considerations. Thus, it seems logical to assume the inflow hydrograph (the design storm) having a peak discharge close to the full capacity Q_o of the conduit. The α -value 0.05 is on the other hand, chosen more arbitrarily. Moreover, if the flow is assumed to be turbulent the dependence of Reynolds number on the friction coefficient is eliminated.

Pipe of constant diameter D, wall roughness k, and slope S_o.

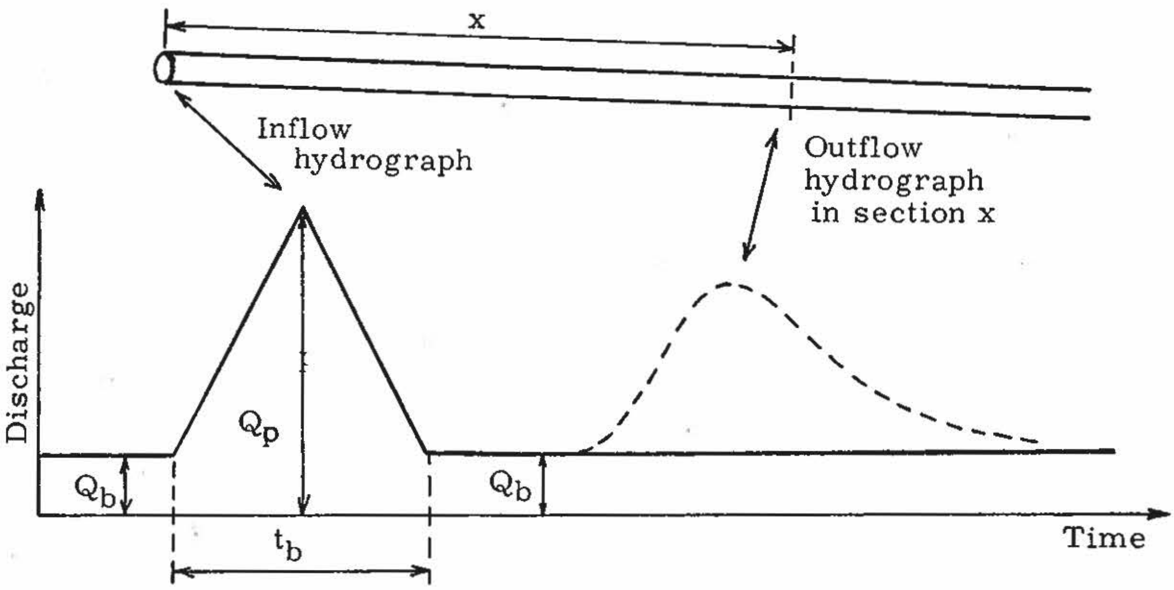

Fig. 3.1 Definition of boundary and initial conditions

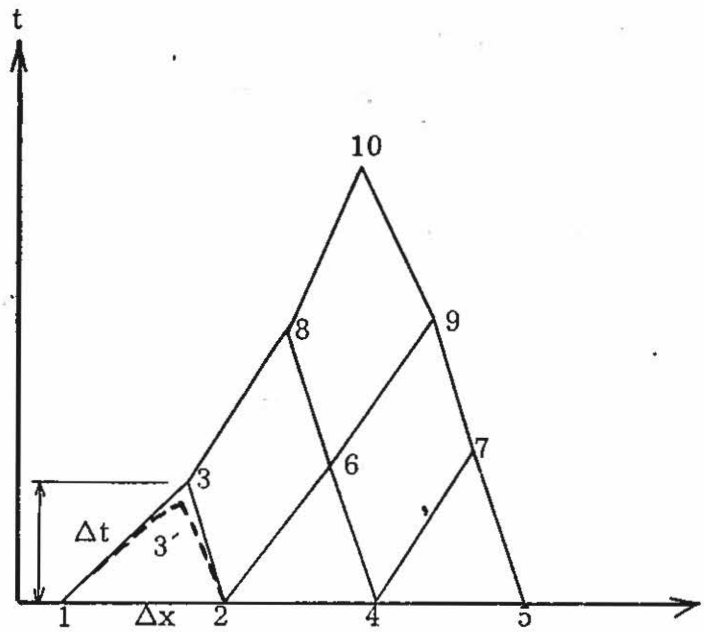

Fig. 3.2 Scheme for numerical computation by the method of characteristics.

The simplification introduced above leads to a reduction from seven to the following four governing parameters

$$F_o;\ S_o;\ (t_b\, V_o/D);\ (k/D); \qquad (3.1.10)$$

Before closing this discussion concerning governing dimensionless parameters, we note that for large values of the channel bottom slope S_o eq. (3.1.6) tends towards the form

$$\frac{\partial Q_x}{\partial x_x} + \frac{\partial A_x}{\partial t_x} = 0;$$

$$S_{fx} = 1; \qquad (3.1.11)$$

(large values of S_o means large values of S_o/F_o^2 as F_o is normally a relatively small quantity). The above equations define the so called "kinematic wave" which is the most simplified model described in this study. For these conditions the three terms accounting for nonuniformity and unsteadiness (in the following called secondary slope terms) on the left hand side of the equation of motion are small compared with the bottom slope S_o. This fact is more evident if the equation is arranged in the form [27].

$$S_f = S_o - \frac{\partial Y}{\partial x} - \frac{1}{2g}\frac{\partial}{\partial x}\left(\frac{Q^2}{A^2}\right) - \frac{1}{g}\frac{\partial}{\partial t}\left(\frac{Q}{A}\right); \qquad (3.1.12)$$

steady uniform flow

steady nonuniform flow

unsteady nonuniform flow

3.2 The method of characteristics

The equation of motion and continuity form a pair of quasi-linear hyperbolic partial differential equations with no general analytical solution. Important information about the properties of these equations is, however, obtained if they are converted into an equivalent pair of ordinary differential equations by the method of characteristics [28].

Written in the form (transformation of eq. (3.1.1) by use of eq. (2.1.12) and the continuity equation)

$$\begin{cases} \dfrac{\partial Q}{\partial x} + \dfrac{\partial A}{\partial t} = 0; \\[2ex] \dfrac{\partial Q}{\partial t} - \dfrac{2Q}{A}\,\dfrac{\partial A}{\partial t} - \left(\dfrac{Q^2}{A^2} - g\dfrac{A}{B}\right)\dfrac{\partial A}{\partial x} = gA\,(S_o - S_f); \end{cases} \tag{3.2.1}$$

the equations of continuity and of motion are quasi-linear in the linear variables Q and A. (They are called quasi-linear though they are non-linear because they may be converted into ordinary differential equations).

We now suppose that Q and A are prescribed at all points along a curve C_o in the xt-plane and that their partial derivatives exist. By definition the partial derivatives must satisfy the equations

$$\begin{cases} \dfrac{dQ}{dt} = \dfrac{\partial Q}{\partial x} \cdot \dfrac{dx}{dt} + \dfrac{\partial Q}{\partial t}; \\[2ex] \dfrac{dA}{dt} = \dfrac{\partial A}{\partial x} \cdot \dfrac{dx}{dt} + \dfrac{\partial A}{\partial t}; \end{cases} \tag{3.2.2}$$

Eq. (3.2.1) and (3.2.2) constitute a system of four linear equations in the four partial derivatives which may be written in the form

$$\begin{bmatrix} 1 & 0 & 0 & 1 \\ 0 & 1 & g\frac{A}{B} - \left(\frac{Q}{A}\right)^2 & - \frac{2Q}{A} \\ dx & dt & 0 & \\ 0 & 0 & dx & dt \end{bmatrix} \begin{bmatrix} \partial Q/\partial x \\ \partial Q/\partial t \\ \partial A/\partial x \\ \partial A/\partial t \end{bmatrix} = \begin{bmatrix} 0 \\ gA(S_o - S_f) \\ dQ \\ dA \end{bmatrix} \tag{3.2.3}$$

We will now try to find out if there exists a curve C_o or a set of curves in the xt-plane along which eq (3.2.3) does not give us a unique solution of the four partial derivatives.

A unique solution is assured unless the determinant of coefficients vanishes, that is, unless

$$\begin{vmatrix} 1 & 0 & 0 & 1 \\ 0 & 1 & g\frac{A}{B} - (\frac{Q}{A})^2 & \frac{2Q}{A} \\ dx & dt & 0 & 1 \\ 0 & 0 & dx & dt \end{vmatrix} = 0; \qquad (3.2.4)$$

By expansion, this equation can be written

$$(\frac{dx}{dt})^2 - \frac{2Q}{A}\frac{dx}{dt} - \left[g\frac{A}{B} - (\frac{Q}{A})^2\right] = 0; \qquad (3.2.5)$$

from which we obtain the two solutions

$$\frac{dx}{dt} = \frac{Q}{A} \pm \sqrt{g\frac{A}{B}}; \qquad (3.2.6\,a,b)$$

The two solutions define two curves along which eq (3.2.3) cannot have a unique solution and hence no solution exists (which we have assumed) unless the numerator determinant of Cramer´s rule vanishes. Thus, if anyone of the columns of the coefficient matrix is replaced by the right hand side of eq (3.2.3) the new matrix must also vanish. That is, if the first column is replaced,

$$\begin{vmatrix} 0 & 0 & 0 & 1 \\ gA(S_o-S_f) & 1 & g\frac{A}{B} - (\frac{Q}{A})^2 & -\frac{2Q}{A} \\ dQ & dt & 0 & 0 \\ dA & 0 & dx & dt \end{vmatrix} = 0; \qquad (3.2.7)$$

or, after expanding

$$\frac{dQ}{dt} - \left[(\frac{Q}{A})^2 - g\frac{A}{B}\right]\frac{dA}{dt}\cdot\frac{dt}{dx} = gA\,(S_o - S_f); \qquad (3.2.8)$$

Thus, along the curve (3.2.6 a) we have the equation

$$\frac{dQ}{dt} - (\frac{Q}{A} - \sqrt{g\frac{A}{B}})\,\frac{dA}{dt} = gA\,(S_o - S_f); \quad \left\{\begin{array}{l}\text{valid for} \\ \frac{dx}{dt} = \frac{Q}{A} + \sqrt{g\frac{A}{B}}\end{array}\right. \qquad (3.2.9\,a)$$

and along the curve (3.2.6b)

$$\frac{dQ}{dt} - \left(\frac{Q}{A} + \sqrt{g\frac{A}{B}}\right)\frac{dA}{dt} = gA\,(S_o - S_f); \quad \begin{cases} \text{valid for} \\ \frac{dx}{dt} = \frac{Q}{A} - \sqrt{g\frac{A}{B}} \end{cases} \qquad (3.2.9\,b)$$

If either eq. (3.2.6a) or (3.2.6b) are satisfied, we will have infinitely many solutions of the partial derivatives, all corresponding to the same prescribed value of Q and A along the curve C_o. The two equations define the so called characteristics of the simultaneous equations (3.2.1)

<u>the forward characteristic, C^+:</u> (eq. (3.2.9a)

<u>the backward characteristic, C^-:</u> eq. (3.2.9b)

The system of partical equations has now been converted into a system of ordinary differential equations valid along certain curves; the characteristics, in the xt-plane. Since the partial equations have two characteristics, they are called hyperbolic.Equations possessing only one characteristic are called parabolic, while elliptic equations have no real characteristics, that is, any possible curve will satisfy the condition for a unique solution of the derivatives.

Analytical solutions of the equations (3.2.9) along the characteristics cannot be obtained. However, the characteristics may be used to find approximate values of Q and A in additional points (x, t), [29].

Consider two points 1 and 2 on the x-axis a small distance Δx apart, fig. 3.2. At these points Q, A, B, S_f and S_o are known. From the points straight lines $dx/dt = Q/A \pm \sqrt{gA/B}$ are drawn until they intersect at point 3. If Δx is chosen sufficiently small it is reasonable to expect that the position of the point 3 is a good approximation to the intersection 3′ of the C^+ - and C^- - characteristics issuing from 1 and 2 respectively, since we are only replacing a short segment of these curves by their tangents. The coordinates of point 3 are defined by

$$\begin{aligned} t_3 &= \left(\frac{dt}{dx}\right)_1 (x_3 - x_1); \\ t_3 &= \left(\frac{dt}{dx}\right)_2 (x_3 - x_2); \end{aligned} \qquad (3.2.10)$$

and the values of Q and A in this point are given by eq. (3.2.9 a and b) with $dQ = Q_3 - Q_1$ and $Q_3 - Q_2$, and $dA = A_3 - A_1$ and $A_3 - A_2$, respectively.

In the same manner the coordinates and the values of Q and A may be determined at points 6, 7 and so on. The characteristic equations are thus of a form that can be solved by digital computers. (For further discussions, see Section 4.2).

It follows from the discussion above that values of Q and A in the bounded region below point P in fig. 3.3 a are completely determined by the initial values on the line KL, or, which is equivalent, conditions at the point P is uniquely determined by the initial conditions on the line KL. The region KPL are called the domain of dependence of point P or the domain of determincay of the segment KL.

Correspondingly we may define the range of influence of a point P as a region of the xt-plane were the solution of the differential equations are influenced by the initial values in P, see fig. 3.3 b. Thus, only disturbances created between K and L on the x-axis may influence the solution in the region bounded by the two curves C^- and C^+ in fig. 3.3 a. Since these curves satisfy eq. (3.2.6) where Q/A is the average flow velocity, $\sqrt{gA/B}$ must represent the speed relative the flowing stream at which a disturbance propagates. The quantity $c_d = \sqrt{gA/B}$ therefore represents the propagation velocity of small disturbances, that is small in the sence that only discontinuities in derivatives occur at the front of a disturbance [29] (infinitely many solutions of the partial derivatives).

If we consider a channel having a rectangular section of constant width the relative propagation speed of a small disturbance is

$$c_d = \sqrt{gY} \tag{3.2.11}$$

which we recognize as the speed of a long wave in water of depth Y. Thus if

$$\text{the Froude number } F = \frac{V}{\sqrt{gA/B}} < 1; \tag{3.2.12}$$

a disturbance will propagate in both the upstream and downstream directions, the flow is subcritical. If $F > 1$, a disturbance will propagate only in the downstream direction and we have supercritical flow. The characteristics corresponding to the conditions $F < 1$, $F = 1$ and $F > 1$ are shown in fig. 3.4.

Disturbances which propagate with the relative velocity $c_d = \sqrt{gA/B}$ are called <u>dynamic waves.</u>

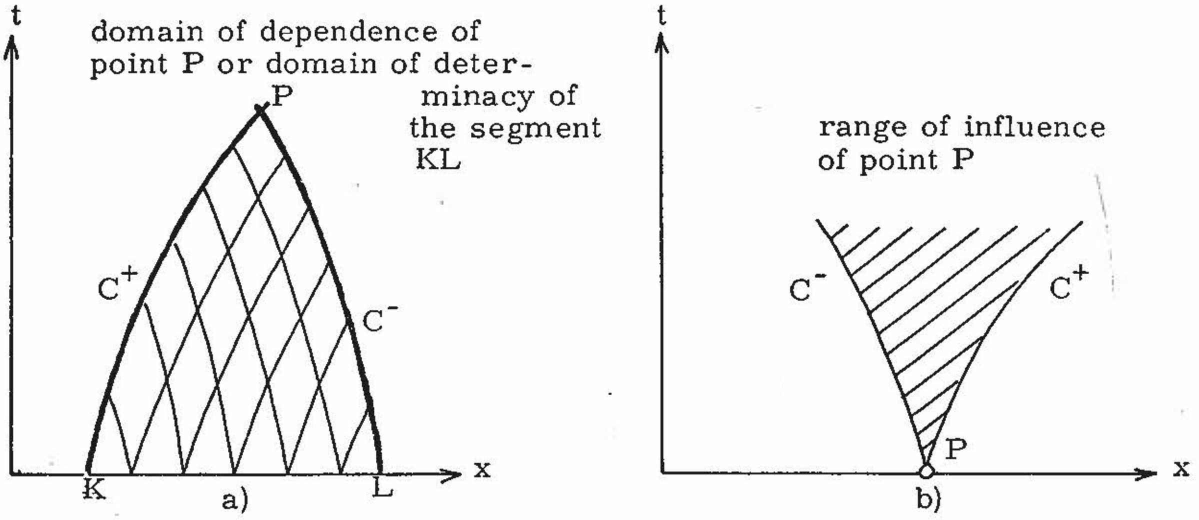

Fig. 3.3 Domain of dependence, determincay and range of influence

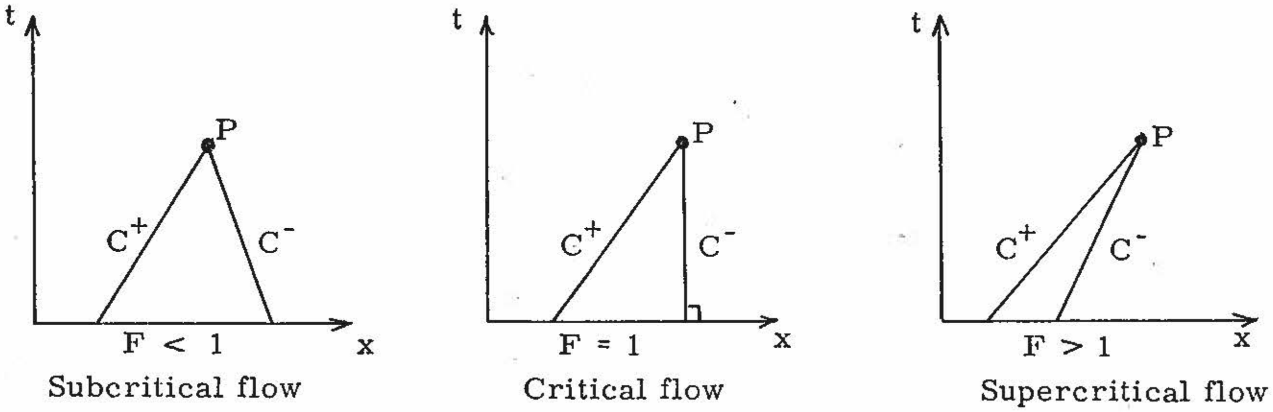

Fig. 3.4 Characteristics corresponding to different values of the Froude number $V/\sqrt{gA/B}$.

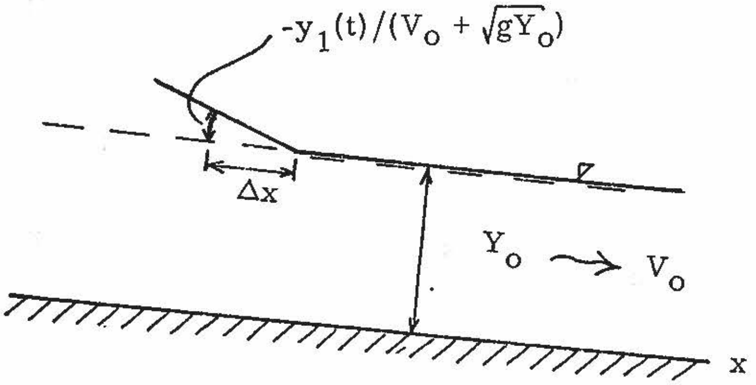

Fig. 3.5 Front of a small disturbance

3.3 Damping of dynamic waves

It may be shown [27], that if bed slope S_o and channel friction S_f are neglected any positive wave, such as an increasing discharge, however, gentle, must eventually form a surge with an abrupt wave front. However, if S_o and S_f are taken into account, a positive wave will attenuate as it moves downstream if certain conditions, corresponding to normal values of flow parameters, are fuilfilled. This can be demonstrated by use of the method of characteristics [27] or from purely algebraic arguments [30], see also [31].

We consider a small positive wave introduced in a stream of uniform depth Y_o and uniform velocity V_o in a rectangular channel. The wave front, which is the first disturbance, then propagates downstream, with the velocity $V_o + \sqrt{gY_o}$ and it will have the locus at $\tau = t - x/(V_o + \sqrt{gY_o})$. Expansions of V and Y about the wavefront give

$$\begin{aligned} V &= V_c + \tau v_1(t) + \tau^2 v_2(t) + \ldots\ldots \\ Y &= Y_o + \tau y_1(t) + \tau^2 y_2(t) + \ldots\ldots \end{aligned} \qquad (3.3.1)$$

where v_1, y_1 etc are functions of t alone representing discontinuities in the partial derivatives at the wave front. Particularly, $\partial Y/\partial t = y_1(t)$ and $\partial Y/\partial x = -y_1(t)/(V_o + \sqrt{gY_o})$. Considering only positive waves, $y_1(t)$ is initially positive.

Substituting eq (3.3.1) into eq (3.1.1) written in the form

$$\begin{aligned} & V\frac{\partial Y}{\partial x} + Y\frac{\partial V}{\partial t} + \frac{\partial Y}{\partial t} = 0; \\ & \frac{1}{g}\frac{\partial V}{\partial t} + \frac{1}{2g}\frac{\partial V^2}{\partial x} + \frac{\partial Y}{\partial x} = S_o - S_f; \end{aligned} \qquad (3.3.2)$$

valid for a rectangular section of constant width, and by using the Darcy-Weissbach equation assuming a broad channel and that the friction coefficient f_o is constant.

$$\left.\begin{aligned} S_f &= \frac{f_o}{4Y} \cdot \frac{V^2}{2g} \\ S_o &= \frac{f_o}{4Y_o} \cdot \frac{V_o^2}{2g} \end{aligned}\right\} \Longrightarrow S_f = \frac{S_o V^2}{F_o^2 Y}; \tag{3.3.3}$$

where $F_o = V_o/\sqrt{gY_o}$, gives after some algebra, setting $\tau = 0$,

$$\frac{dy_1}{dt} = \frac{3 y_1^2}{2 Y_o (1 + F_o)} - \frac{g S_o}{V_o} (1 - \tfrac{1}{2} F_o) y_1; \tag{3.3.4}$$

where $dy_1, /dt$ is the growth rate of the discontinuity at the wave front.

It follows from eq (3.3.4) that, if $F_o > 2$, y_1 increases without limit. Since y_1 is proportional to $\partial Y/\partial x$, this means that the wave front becomes vertical and the wave breaks in a bore.

If $F_o < 2$, we have two possibilities. If $y_1(0) > K$, that is $\partial Y/\partial t \ (t = 0) > K$, where

$$K = \left(\frac{g Y_o S_o}{3 V_o}\right) (2 - F_o) (1 + F_o); \tag{3.3.5}$$

again a bore will form. If $y_1(0) = y_o < K$ then y_1 tends to zero. Integration of eq (3.3.4) gives

$$y_1 (t) = \frac{y_o K e^{-t/b}}{K - y_o(1 - e^{-t/b})}; \tag{3.3.6}$$

where $1/b = gS_o(2 - F_o)/2V_o$. Dynamic waves are thus rapidly damped out if $F_o < 2$, $y_o < K$.

The damping mechanism is governed by the magnitude of

$$\frac{t}{b} = \frac{tg S_o (2 - F_o)}{2 V_o} \tag{3.3.7}$$

Substitution of the dimensionless time variable $t_x = t V_o/Y_o$ shows that the decay of the dynamic wave will be governed by the parameter

$$\frac{S_o}{F_o^2} (1 - \frac{F_o}{2}); \tag{3.3.8}$$

which is a combination of the two governing parameters S_o and F_o obtained in section 3.1 by writing the equations of motion and of continuity in non-dimensional form.

It should be emphasized that the discussion above is limited to small disturbances close to the wave front. However, the result obtained may be used as an indicator of the behavior of a positive wave and as an aid for testing of experimental data.

3.4 Kinematic waves

Of most interest from engineering point of view is the behaviour of the wave as a whole. The understanding of the complete wave phenomenon has been very much improved by the studies of Lighthill and Whitham [30], which provided better insight into possible wave types and their properties.

If secondary slope terms, that is terms accounting for non-uniformity and unsteadiness on the right hand side of the equation of motion (3.1.12) are small compared to the bottom slope S_o, the discharge Q is a function of Y alone. Using the Darcy-Weissbach equation, we obtain for a given value of S_o

$$S_f = S_o \Rightarrow Q = A\sqrt{\frac{8gS_oR}{f}} = Q\,(Y); \qquad (3.4.1)$$

assuming f to be a function of Y alone. The equation of continuity

$$\frac{\partial Q}{\partial x} + B\frac{\partial Y}{\partial t} = 0;$$

may then be written

$$\frac{1}{B}\frac{dQ}{dY}\cdot\frac{\partial Y}{\partial x} + \frac{\partial Y}{\partial t} = 0; \qquad (3.4.2)$$

If we note that by definition

$$\frac{dY}{dt} = \frac{\partial Y}{\partial x}\cdot\frac{dx}{dt} + \frac{\partial Y}{\partial t}; \qquad (3.4.3)$$

a comparison of the two realtions (3.4.2) and (3.4.3) shows, that if

$$\frac{dx}{dt} = \frac{1}{B}\frac{dQ}{dY} \Rightarrow \begin{cases} \dfrac{dQ}{dt} = 0; \\ \dfrac{dY}{dt} = 0; \end{cases} \qquad (3.4.4)$$

This means that Q and Y appear to have constant values by an observer moving with the velocity dx/dt given by eq (3.4.4). We have thus demonstrated the existance of a wave, the properties of which follow from the equation of continuity. Accordingly, Lighthill and Whitham described this wave as "kinematic" in contrast to dynamic waves, depending on the complete equations of continuity and motion.

As the secondary slope terms are never totally negligible, dynamic waves always occur and we always have a "competition between kinematic and dynamic waves" [30]. This competition may be described as in fig. 3.6.

In a wide rectangular channel with constant friction coefficient, the kinematic wave velocity c is

$$c = \frac{1}{B}\frac{dQ}{dY} = \frac{1}{B}\frac{d}{dY}\left[BY\sqrt{\frac{8gS_oY}{f}}\right] = \frac{3}{2}\sqrt{\frac{8\,gS_oY}{f}} = \frac{3}{2}\,V; \qquad (3.4.5)$$

where V is the average velocity, while the speed of a dynamic wave is

$$V \pm c_d = V \pm \sqrt{gY} \qquad (3.4.6)$$

Thus, if $F = V/\sqrt{gY} < 2$, a condition which will normally be fullfilled, the speed of the kinematic wave is less than the speed of the dynamic wave and the dynamic wave acts as forerunner of the main wave. However, as found in section 3.3, the decay of the dynamic wave is exponential unless the initial rate of growth exceeds the value K, given by eq (3.3.5). The main body of the wave therefore moves primarily as a kinematic wave, even if the kinematic character will be modified by the influence of secondary slope terms. This kinematic character has also been indicated by Lighthill and Whitham, using a linear theory of small disturbances [30].

As a purely kinematic wave moves downstream, the wave front becomes steeper because the wave velocity increases with depth, fig. 3.7. The wave is thus distorted but it maintains its maximum depth and maximum discharge. Under certain conditions, the steepening of the wave front will lead to the formation of a surge, that is, the wave will break.

However, as the wave front becomes steeper the wave can no longer be regarded as a purely kinematic wave but also dynamic properties (secondary slope term) have to be considered. The effect of the secondary slope terms is a flattening of the wave. The steepening of the wave front will be retarded

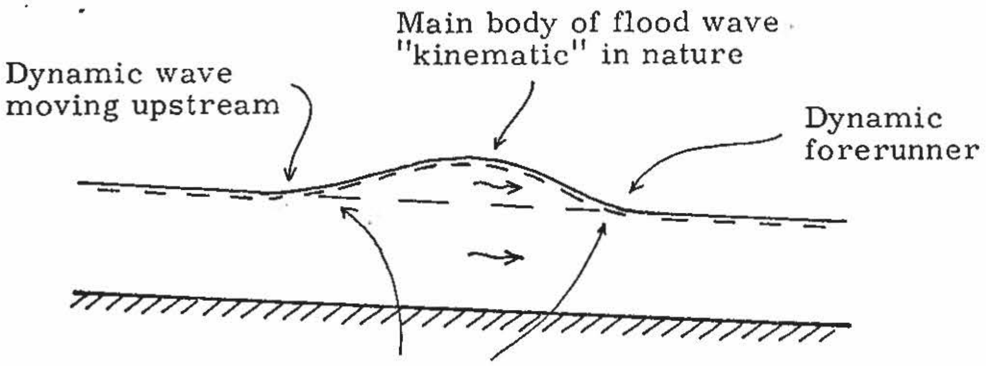

Fig. 3.6 "Competition" between kinematic and dynamic waves, [30, 27]

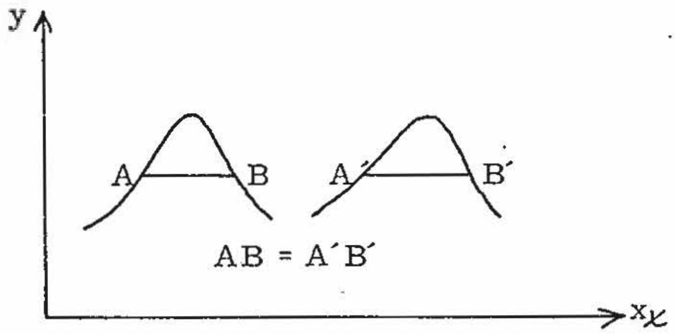

Fig. 3.7 Distortion of a kinematic wave

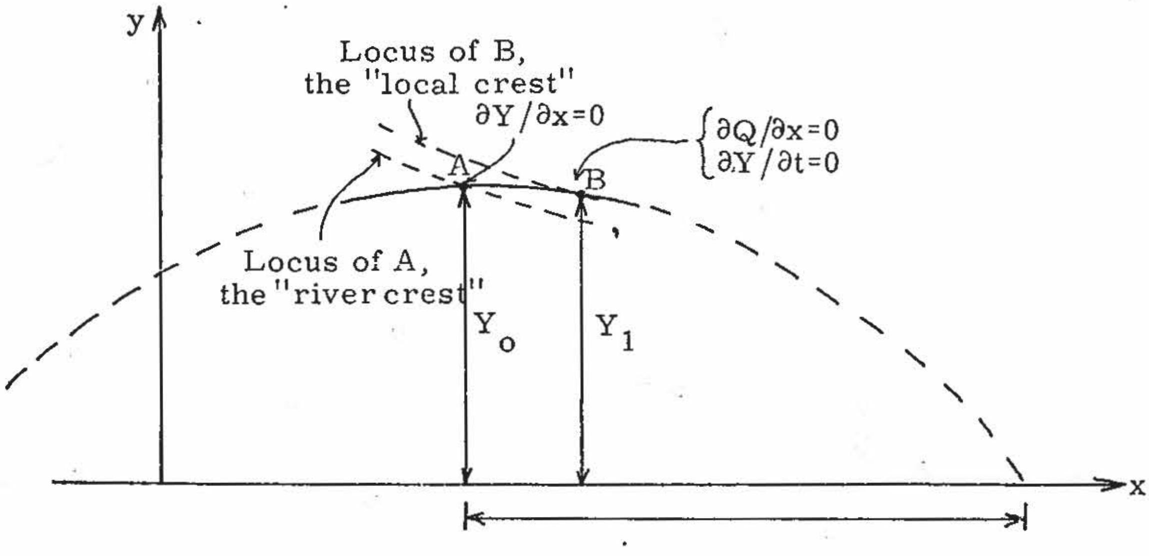

Fig. 3.8 Profile of non-kinematic wave as assumed by Henderson [27]

and the formation of a surge will eventually be prevented. If the flattening effect equals the kinematic steepening a steady profile may be obtained. Such a wave, normally called "monoclinical" was in ref. [30] given the name "kinematic shock".

The possibility of occurence of kinematic and monoclinical type waves in nature is discussed in [27]. According to this study, monoclinical waves are not likely to occur unless in very long rivers.

Kinematic waves may occur if the bottom slope is large compared to other slope terms. However, the secondary slope terms will always modify the wave. The velocity of the crest may then differ from the kinematic value and the wave crest will subside, see section 3.5.

3.5 Subsidence of the flood crest. The speed of a subsiding flood wave.

The subsidence of a kinematic wave is a function of the relative influence of the secondary slope terms in the equation of motion

$$V = \left(\frac{8gY}{f}\right)^{1/2} \left(S_o - \frac{\partial Y}{\partial x} - \frac{1}{2g}\frac{\partial V^2}{\partial x} - \frac{1}{g}\frac{\partial V}{\partial t}\right)^{1/2}; \tag{3.5.1}$$

in proportion to the influence of the bottom slope S_o. This has been discussed by Henderson [27, 32], who considered a wide rectangular channel and a given inflow hydrograph $q = q(t)$.

For a kinematic wave profile we have by definition

$$\frac{dY}{dt} = \frac{\partial Y}{\partial t} + c\frac{\partial Y}{\partial x} = 0; \tag{3.5.2}$$

The magnitude of $\partial Y/\partial x$ relative S_o is then

$$\begin{aligned} -\frac{\partial Y/\partial x}{S_o} &= \frac{1}{cS_o}\cdot\frac{\partial Y}{\partial t} = \frac{2}{3(YS_o)^{1/2}S_o}\cdot\frac{\partial Y}{\partial t} \propto \\ &\propto \frac{1}{YS_o^2}\cdot\frac{\partial q}{\partial t} \propto \frac{1}{(qS_o)^{2/3}S_o}\cdot\frac{\partial q}{\partial t}; \end{aligned} \tag{3.5.3}$$

as $q \propto Y^{3/2} S_o^{1/2}$. The term $(\partial q/\partial t)q^{2/3}$ depends on the inflow hydrograph alone, why the term $(\partial Y/\partial x)/S_o$ must become small as S_o increases.

We also find that

$$\frac{1}{2g} \frac{\partial V^2}{\partial x} / \frac{\partial Y}{\partial x} = O(F^2);$$

$$\frac{1}{g} \frac{\partial V}{\partial t} / \frac{\partial Y}{\partial x} = \frac{c}{g} \frac{\partial V}{\partial x} / \frac{\partial Y}{\partial x} = \frac{3}{4g} \frac{\partial V^2}{\partial x} / \frac{\partial Y}{\partial x} = O\,(F^2); \qquad (3.5.4)$$

where F is the Froude number and O ( ) is the Ordo symbol which means "is of order of magnitude of".

This order of magnitude analysis leads to the definition of three classes of flood waves:

- flood waves on gentle slopes: channels with sufficiently gentle slope, $F^2 \ll 1$

  $$V \propto Y^{1/2} \left(S_o - \frac{\partial Y}{\partial x}\right)^{1/2};$$

- flood waves on intermediate slope:

  $$V \propto Y^{1/2} \left(S_o - \frac{\partial Y}{\partial x} - \frac{1}{2g} \frac{\partial V^2}{\partial x} - \frac{1}{g} \frac{\partial V}{\partial t}\right)^{1/2} \quad ;$$

- flood waves on steep slopes: channels with steep slopes, excluding the case of torrential (torrential = $F^2 \gg 1$)

  $$V \propto Y^{1/2} S_o^{1/2} \qquad \text{(kinematic wave, non subsiding)}$$

The subsidence of the first two classes of waves has been discussed in[27, 32] assuming the wave crest defined by a parabola. The main conclusions, which are true only for long waves, are

- The peak of discharge at a particular section occurs earlier than the peak of depth. The wave crest should then be defined as the point B in fig. 3.8. This definition corresponds to the maximum level reached at any particular section.

- The subsidence of the local wave crest B is given by

$$\frac{dY_1}{dx} = \frac{Y_o}{3 S_o c_o^2} \cdot \frac{\partial^2 Y}{\partial t^2} \cdot (1 - \frac{F_1^2}{4}); \qquad (3.5.5)$$

where index "1" refers to the local wave crest B.

- The speed of the subsiding wave differs only in second order terms from the kinematic wave speed.

The assumptions involved imply that the two last statements are true only for mild, slow-rising waves. However, substitution of the dimensionless variables defined by eq (3.1.4) exchanging D for Y_o, again gives the two governing parameters S_o and F_o found in section 3.1 and 3.3.

Equation (3.5.5) may be written ($kc_o = \partial^2 Y/\partial t^2$)

$$\frac{dY_1}{dx} = -\frac{kY_o}{3 S_o} (1 - \frac{F_1^2}{4}) ; \qquad (3.5.6)$$

where k is a function of time alone ($k > 0$) defining the parabola AB in fig. 3.8,

$$Y = Y_o - \frac{kx^2}{2}; \qquad (3.5.7)$$

If k and F_1 as a first approximation are assumed constant and equal k(0) and F_o, respectively, integration of eq (3.5.6) gives

$$Y_1 = Y_o(0)\ e^{-\frac{xk(0)}{3 S_o}(1 - \frac{F_o^2}{4})} ; \qquad (3.5.8)$$

suggesting an exponential decay of the crest depth with distance. This is true, certainly, only if $xk(1 - F_1^2/4)$ increases with x. However, it is believed that k and F_1 are weak functions of t, i.e. they vary slowly as the wave progresses.

3.6 Diffusion of kinematic waves

For flood waves on gentle bottom slopes ($F^2 \ll 1$) the decay of a kinematic wave may be described by a diffusion type of equation obtained by transformation of the relations presented in the foregoing sections, valid for a wide rectangular channel.

$$Q = BY \sqrt{\frac{8gY}{f} \left(S_o - \frac{\partial Y}{\partial x}\right)}$$

$$c = \frac{3V}{2} = \frac{3}{2} \sqrt{\frac{8gY}{f} \left(S_o - \frac{\partial Y}{\partial x}\right)} \tag{3.6.1}$$

$$\frac{\partial Q}{\partial x} + B \frac{\partial Y}{\partial t} = 0$$

Differentiating the first relation and substituting the second, we have

$$\frac{\partial Q}{\partial x} = B \frac{\partial Y}{\partial x} \cdot c - \frac{BYc}{3\left(S_o - \frac{\partial Y}{\partial x}\right)} \cdot \frac{\partial^2 y}{\partial x^2} \tag{3.6.2}$$

The third relation then leads to the result

$$\frac{\partial Y}{\partial t} + c \frac{\partial Y}{\partial x} = K \frac{\partial^2 y}{\partial x^2} \tag{3.6.3}$$

where $K = \dfrac{Yc}{3\left(S_o - \frac{\partial Y}{\partial x}\right)}$

As $c = dx/dt$, eq. (3.6.3) may be written

$$\frac{dY}{dt} = K \frac{\partial^2 y}{\partial x^2} \tag{3.6.4}$$

which has the same form as the diffusion equation with constant diffusion coefficient K. Eq. (3.6.4) may also be considered as the standard wave equation, containing an extra diffusion term $K\, \partial^2 y/\partial x^2$. [27].

If K and c_k are assumed constant, eq (3.6.4) can be solved explicitly. For a unit rise Δy_1 and a duration $t_1 - t_2 = t_o$ of the rise Hayami[33, 27] obtained

$$\frac{\Delta y_2}{\Delta y_1} = \frac{2}{\sqrt{\pi}} \int_{\xi_1}^{\xi_2} \exp\left[\frac{cx}{2K} - \xi^2 - \left(\frac{cx}{4K\xi}\right)^2\right] d\xi \qquad (3.6.5)$$

where Δy_2 is the rise at section x, $\xi_1 = x/2\sqrt{Kt}$, and $\xi_2 = x/2\sqrt{Kt_2}$. This solution indicates again an exponential decaying amplitude - the classical solution to the diffusion problem.

The evolution of the integral in eq (3.6.5), which is valid only for a wide rectangular channel, has to be carried out numerically. Furthermore, as the "diffusion coefficient" K and the kinematic velocity c will be functions of x and t, the integration has to be carried out stepwise in the downstream direction.

For a circular **cross section** eq (3.6.4) has no explicit solution. A solution can thus be obtained only by numerical methods. However, as eq (3.6.4) does not take into account the last two secondary slope terms of eq (3.5.1) it is of less practical interest. A numerical solution can as easily be obtained for the complete governing equations.

4. DESCRIPTION OF METHODS FOR FLOOD ROUTING IN STORM DRAINS

4.1 Introduction

Flood routing models presented in literature, applicable to storm drains, may be divided in two groups

(a) models, which give an adequat simulation of unsteady free surface flow, including simulation of transient backwater conditions.

(b) models, where hydrographs are routed independently of downstream conditions.

An accurate simulation of transient backwater conditions is not possible without an exact solution of the Saint-Venant equations simultaneously throughout the sewer system. The only storm drain model, which to the writers knowledge might have such a routing routine, is the Dorsch-model [5]. However, available information does not make it possible to draw any definitive conclusions about the properties of this model.

Examples of the second type (type b) of models are the EPA-model [3], the NIVA-model [1, 2], the RRL-method [7, 11] and models built on the kinematic wave theory [6, 9]. In all these models the hydrograph is routed step-wise through the sewer system independently of downstream conditions, that is independently of backwater effects due to ponding as a result of flow control structures or lateral inflow in junction boxes.

The advantage of this procedure is that it is less complicated and that it permits a succesive design of the drainage system. It is thus possible to introduce in the type b model a subroutine which finds the smallest necessary pipe dimension for given values of slope and length of the sewer line.

Neglecting backwater effects may under certain conditions be a serious drawback. However, certain backwater effects may be simulated in an approximate way by built in storage routines.

4.2 Numerical solutions of the Saint Venant equations

An accurate simulation of transient backwater conditions requires a solution of the complete Saint-Venant equations or the characteristic equations simultaneously throughout the sewer system. Unfortunately, solutions must be obtained by numerical procedures.

Present-day numerical solutions appear, by and large, to fall into one of the following categories:

- computation along characteristics
- computation with explicit scheme
- computation with implicit scheme

These three techniques will be presented briefly below. The discussion is based on the Saint-Venants equations written in the form

$$\frac{\partial Q}{\partial x} + \frac{\partial A}{\partial t} = 0;$$
$$\frac{\partial Q}{\partial t} - \frac{2Q}{A}\frac{\partial A}{\partial t} - \left(\frac{Q^2}{A^2} - g\frac{A}{B}\right)\frac{\partial A}{\partial x} = gA(S_o - S_f) \qquad (4.2.1)$$

and the characteristic equations

$$C^+: \quad \frac{dQ}{dt} - \left(\frac{Q}{A} - \sqrt{g\frac{A}{B}}\right)\frac{dA}{dt} = gA(S_o - S_f) \qquad (4.2.2a)$$

$$C^-: \quad \frac{dQ}{dt} - \left(\frac{Q}{A} + \sqrt{g\frac{A}{B}}\right)\frac{dA}{dt} = gA(S_o - S_f) \qquad (4.2.2b)$$

4.2.1 Computation along characteristics

This procedure has already been discussed in chapter 3.2 where we have shown, see fig. 3.2, that it is necessary to calculate not only the values of the unknown functions Q and A, but also the values of the coordinates (x, t) of the points themselves in the xt-plane. The results are thus obtained for odd times and distances and some interpolation of the result is required. It would be more convenient to use a fixed rectangular net in the x, t-plane requireing the calculation of Q and A only, and having the advantage of furnishing these values at a convenient set of points. This can be arrived at by using the so called method of characteristics with specified intervals, see for instance [15, 34, 35]. In this method, Q and A at point P in the x, t-plane of fig. 4.1 are computed from known values at points M, R and L using the characteristic equations (4.2.2) under the assumption that Δt is sufficiently small so that the characteristics PE and PF are considered straight lines and that E and F fall within the interval ML. Hence, the value of Δt must satisfy the so called Courant condition

$$\Delta t \leqslant \frac{\Delta x}{V + \sqrt{gA/B}}; \tag{4.2.3}$$

The coordinates of E and F are first determined from the relations

$$\begin{aligned} x_E &= x_P - \Delta t\,(V + \sqrt{gA/B})_R; \\ x_F &= x_P + \Delta t\,(V - \sqrt{gA/B})_R; \end{aligned} \tag{4.2.4}$$

The values of Q_E and Q_F are, assuming subcritical flow, evaluated by linear interpolation within the intervals MR and RL, respectively (the same for A_E and A_F)

$$\begin{aligned} Q_E &= Q_M + \frac{Q_R - Q_M}{\Delta x}\,(x_E - x_M) \\ Q_F &= Q_L + \frac{Q_R - Q_L}{\Delta x}\,(x_L - x_F) \end{aligned} \tag{4.2.5}$$

Then, with the derivatives written as

$$\begin{aligned} C^+: \quad \frac{dQ}{dt} &= \frac{1}{\Delta t}\,(Q_P - Q_E) \\ C^-: \quad \frac{dQ}{dt} &= \frac{1}{\Delta t}\,(Q_P - Q_F) \end{aligned} \tag{4.2.6}$$

and correspondingly for A, we have after substitution in eq. (4.2.2) if S_f is expressed in the known values Q_E, A_E and Q_F, A_F, respectively, two equations, which can be solved for the two unknowns Q_P and A_P. Thus, if Q and A are known for all x at time t new values of Q and A can be obtained at time $t + \Delta t$ for the same x-points.

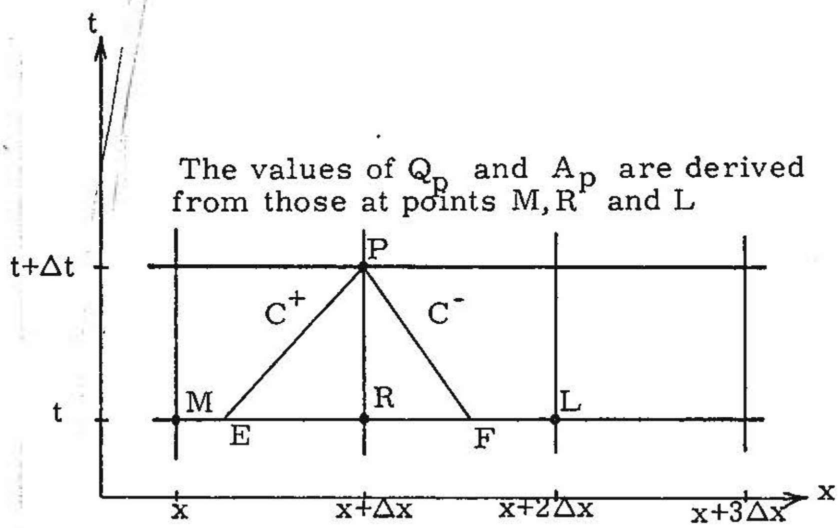

Fig. 4.1 Computation by the Method of Characteristics with Specified Intervals

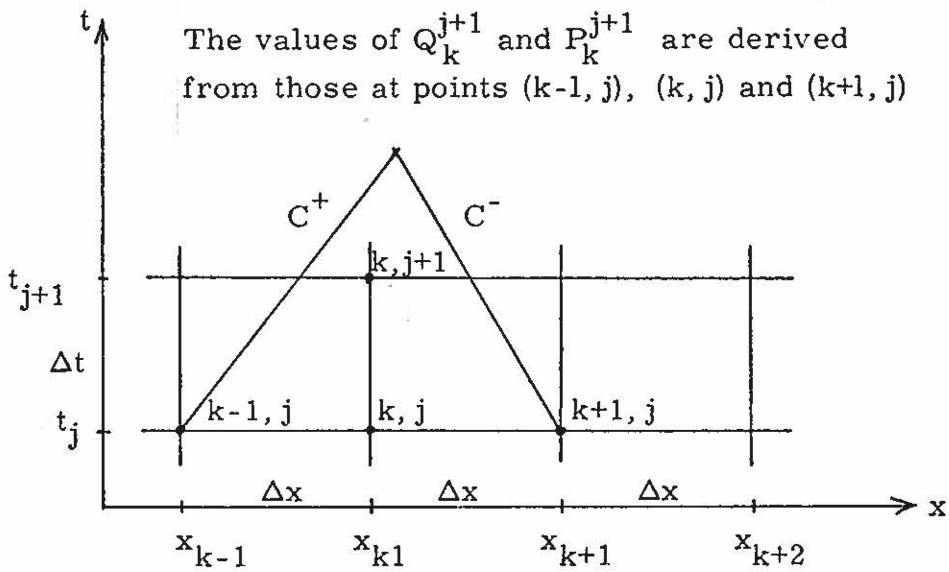

Fig. 4.2 Computation with explicit scheme.

To solve for the upstream and downstream boundary the boundary conditions have to be introduced. The upstream boundary condition is the inflow hydrograph $Q = Q(t)$, which after substitution in eq. (4.2.2b) gives the unknown variable A. The downstream boundary condition may for instance be the depth-discharge relation given by the critical depth at a free outfall which together with eq. (4.2.2a) determines the two unknowns.

4.2.2 Computation with explicit scheme

The numerical technique presented below consists in replacing the partial derivatives in the Saint-Venant equations or in the characteristic equations by finite difference quotients in a fixed rectangular net of the xt-plane. With reference to fig. 4.2 a first order approximation of the space derivatives in the neighbourhood of point (x_k, t_j) is [36].

$$\frac{\partial Q}{\partial x} \approx \frac{Q^i_{k+1} - Q^i_k}{\Delta x} \approx \frac{Q^i_k - Q^i_{k-1}}{\Delta x} \approx \frac{Q^i_{k+1} - Q^i_{k-1}}{2\Delta x}; \text{etc.} \qquad (4.2.7)$$

and of the time derivatives

$$\frac{\partial Q}{\partial t} \approx \frac{Q^{j+1}_k - Q^j_k}{\Delta t} \approx \frac{Q^{j+1}_k - Q^{j-1}_k}{2\Delta t}; \text{ etc.} \qquad (4.2.8)$$

and of the coefficients

$$\left(\frac{Q}{A}\right)^{j+1}_k \approx \left(\frac{Q}{A}\right)^j_k \approx \frac{1}{2}\left[\left(\frac{Q}{A}\right)^{j+1}_k + \left(\frac{Q}{A}\right)^j_k\right]; \text{ etc.} \qquad (4.2.9)$$

The way in which the partial derivatives and the coefficients are evaluated determines the type of difference scheme. It also determines whether a scheme will be conditionally stable, unconditionally stable, or always unstable. A stable finite-difference scheme means , a scheme, in which small numerical errors of truncation and round-off are not amplified during successive applications of the procedure. Investigations of the stability of a numerical scheme may be made using the von Neumann technique [36, 37] or the matrix method [38]. However, as the stability investigation has to be carried out for a simplified version of the given system of equations, for example a linearized form, this investigation can serve only as a quide and it has to be completed with computational trials [39].

In the situation of fig. 4.2, we assume that Q and A are known for all x on line tj. The values of Q and A for (k, j+1) can then be calculated using the Saint-Venant equations, eq. (4.2.1). The derivatives are then replaced by the following differences

$$\frac{\partial Q}{\partial t} = Q_k^{j+1} - Q_k^j \; ; \quad \frac{\partial A}{\partial t} = A_k^{j+1} - A_k^j$$
$$\frac{\partial Q}{\partial x} = \frac{Q_{k+1}^j - Q_{k-1}^j}{2\,\Delta x} \; ; \quad \frac{\partial A}{\partial x} = \frac{A_{k+1}^j - A_{k-1}^j}{2\,\Delta x} \qquad (4.2.10)$$

If the coefficients are evaluated in point (k, j) substitution of the finite differences in eq. (4.2.1) again give two equations from which the unknowns Q_k^{j+1} and A_k^{j+1} can be solved explicitely. Thus, if Q and A are known for all x on line t_j, values of Q and A on line t_{j+1} can be calculated by successive application of these equations. (The procedure described in section 4.2.1, which also leads to an explicit solution of Q and A in point (k, j+1), may also be characterized as computation with explicit scheme). Boundary conditions are introduced as in section 4.2.1.

Explicit schemes can also be based on the characteristic equations [29, 36]. The partical derivatives may be evaluated in a more or less approximative way leading to different numerical algorithms, for example the diffusing scheme and the Lax-Wendroff scheme [34].

The stability of an explicit scheme is - if the scheme is at all stable - always governed by the Courant condition. That is, once Δx is chosen, Δt must satisfy eq. (4.2.3). Stable explicite schemes based on staggered nets in the xt-plane are reported in ref. [36, 48].

Though the explicit schemes imply a determination of the unknowns in only one point at a time, this technique gives a simultaneous solution throughout the system due to the introduction of the Courant condition. This condition limits the time step so that the point (k, j+1) is always within the domain of determinacy of the segment (k-1, j) - (k+1, j), see fig. 3.3a.

4.2.3 Computation with implicit scheme

In explicit schemes partial x-derivatives are evaluated on the "known" time line t_j. In implicit schemes these derivatives are evaluated on line t_{j+1}. For example

$$\frac{\partial Q}{\partial x} \approx \frac{Q_{k+1}^{j+1} - Q_{k-1}^{j+1}}{2\,\Delta x}\;; \qquad (4.2.11)$$

Partial time derivatives are approximated as before. These leads to pair of resulting algebraic equations at each k-point containing six unknowns, on the line j_{j+1}; Q_{k-1}, A_{k-1}; Q_k, A_k, Q_{k+1}, A_{k+1} (thus the designation "implicit"). With two equations for each interior point k = 2 to k = N-1, see fig. 4.3, we then have a system of 2N - 2 equations in 2N unknowns. If the system is completed with the two known boundary conditions and a finite difference form of the backward characteristic equation at the left boundary (k = 1) and of the foreward characteristic equation at the right boundary (k = N), the 2N unknowns may be solved simultaneously on line t_{j+1}.

The obtained system of algebraic equations will be linear if the coefficients in the original equations are evaluated on line t_j. According to [36], such a scheme, based on the Saint-Venant equations (4.2.1), are unconditionally stable if the friction slope S_f is taken on the line t_{j+1}. This can be done, without spoiling the linearity of the system, by local linearization of S_f [36], which may be written

$$S_f = \frac{Q^2}{K^2} \qquad (4.2.12)$$

in which the conveyance $K = 8gA^2R/f$ for a given pipe is a function of A alone. Thus

$$S_{f_k}^{j+1} \approx S_{f_k}^{j} + \left[\frac{\partial S_f}{\partial Q}\right]_k^j (Q_k^{j+1} - Q_k^j) + \left[\frac{\partial S_f}{\partial K}\right]_k^j \left[\frac{\partial K}{\partial A}\right]_k^j (A_k^{j+1} - A_k^j); \qquad (4.2.13)$$

Another stable implicit scheme is presented and exemplified in ref. [40].

The unconditional stability of the implicit schemes means that the numerical procedure is stable for all sizes of time increment. The number of time increments used to cover a hydrograph of interest can thus be reduced. This is done, however, at the expense of solving large systems of linear algebraic equations.

Each pair of resulting algebraic equations contain 6 unknowns. For N x-points a system of 2N equations has to be solved.

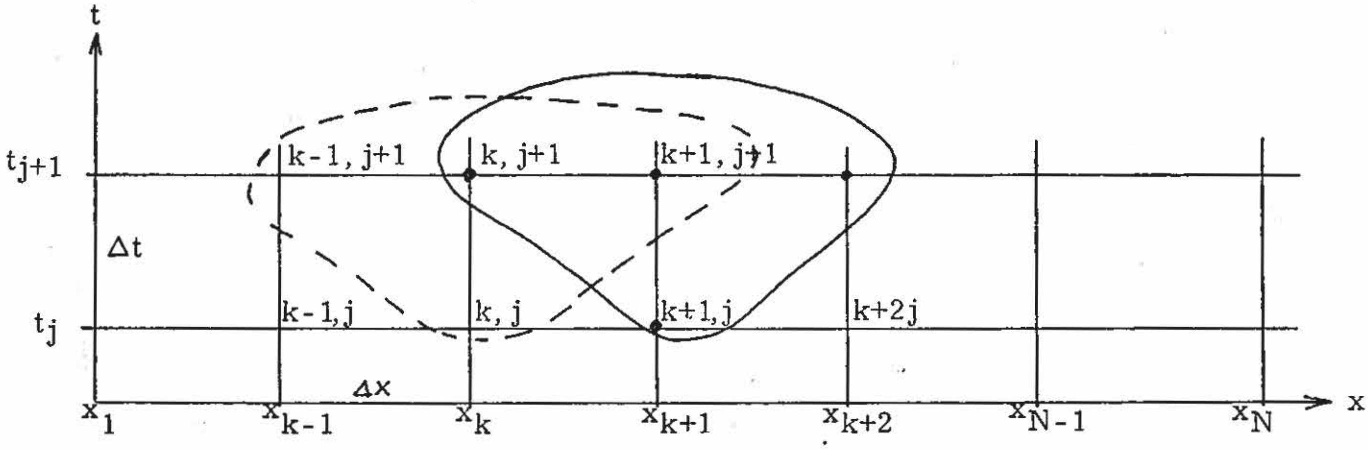

Fig. 4.3 Computation with implicit scheme.

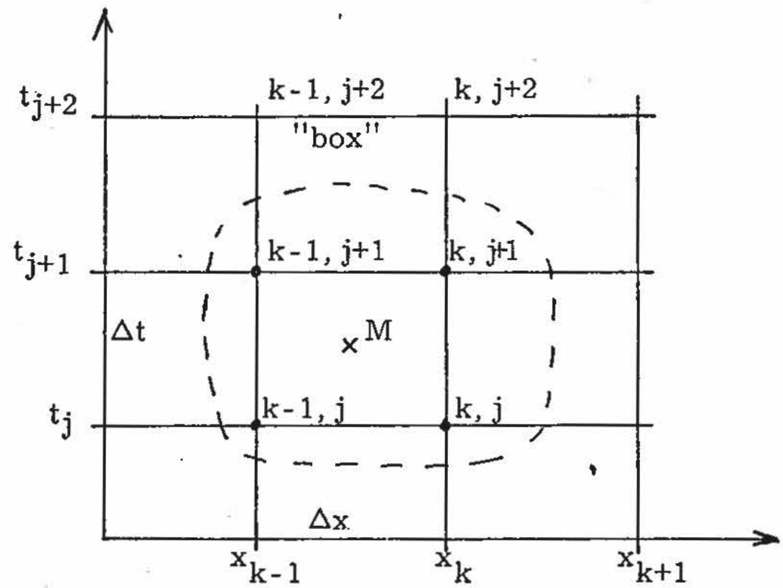

Fig. 4.4 The centered box-scheme.

If also the other coefficients in the original equations are taken on the line t_{j+1}, the system of equations will be non-linear in Q and A [41], and the solution technique will be more complicated and timeconsuming. However, this might be compensated for by a reduction of the time increment due to better approximation of coefficients.

4.2.4 Summary

The method of characteristics with specified intervals and computation with an explicit scheme are characterized by the solution of a large number of simple equations. Each time, the unknowns are determined at only one point in the x, t-plane. The time step Δt is restricted by the Courant condition, eq. (4.2.3).

Computation with an implicit scheme is characterized by the solution of a smaller number of more complex equations. For certain implicit schemes stability of the numerical process is at hand regardless of the time step Δt. However, the values of Δt and Δx cannot be chosen arbitrarily. Too large values may lead to deviations between the solution of the resulting algebraic equations and the solution following the original differential equations. Relatively small time steps and length steps are thus required to obtain a good reproduction of steep hydrographs. Special studies have to be undertaken to obtain criteria for the choice of Δx and Δt.

Usually, difference-schemes are based on equal steps Δx, which may be inconvenient for sewer networks. For the implicit method this can be dealt with by using the so called box-scheme [41] presented in section 4.3 or by a schematization of the system in branches and nodes [42, 47].

Almost all numerical methods presented in literature concern problems related to rivers and canals with, compared to those occurring in storm drains, relatively small and gentle hydrographs. Computational experience shows that the three methods presented above, all give the same accuracy, provided that time steps and length steps are properly chosen. Predicted and observed hydrographs or flood waves have been found to be in good agreement [13, 14, 15, 41, 44].

It is not possible to predict in advance which of the models that will give the most economic computation. This has to be investigated separately for each specific problem. However, some authors [36, 41] claim that explicit methods in many instances result in uneconomic computation due to the large number of timesteps required to ensure numerical stability of the procedure.

The only detailed report concerning flow in storm drains seems to be ref. [12] based on the method of charcteristic with specified intervals. Calculated and measured hydrographs were found to be in good agreement.

If the drainage system is initially dry a special starting method must be used for all procedures described above, except for the non-linear implicit scheme. This is due to the fact that all coefficients in the equations equal zero. However, it is often justified to use a constant base flow as starting condition.

A simultaneous solution of the complete Saint-Venant equations throughout the sewer system is the only way to obtain an accurate simulation of unsteady free-surface flow in storm drains in case of backwater effects. However, complete boundary conditions, for instance multi-junctions, makes the programming difficult and the computing costs high. This is probably the reason why all urban runoff models known to the author (with reservation for ref [5]) are based on a "type b" routing technique described in the following sections.

It is believed by the author that "exact" solutions obtained by the method of characteristics or by computation with explicit or implicit schemes may serve as a basis of comparison of the "type b" models.

4.3 The EPA-transport model and the CTH-transport model

In the EPA (U.S. Environmental Protection Agency)-transport model [3], as well as in the other routing models presented below, the hydrograhps are routed independently of downstream conditions.

The EPA-model is based on the box-scheme [41], even if this fact is not mentioned in the report. In this scheme a centered approximation of spatial and time derivatives are used, see fig. 4.4.

$$\left(\frac{\partial A}{\partial t}\right)_M \approx \frac{(1-w_t)(A_k^{j+1} - A_k^j) + w_t\,(A_{k-1}^{j+1} - A_{k-1}^j)}{\Delta t}\;;$$

$$\left(\frac{\partial A}{\partial x}\right)_M \approx \frac{(1-w_x)(A_k^{j} - A_{k-1}^j) + w_x\,(A_{k}^{j+1} - A_{k-1}^{j+1})}{\Delta x}\;; \qquad (4.3.1)$$

where w_t and w_x are weighting factors [38, 40, 42] which, to ensure stability of the finite difference scheme, have to be chosen somewhat greater than 0.5.

The equation of continuity is then (for simplicity $w_t = w_x = 0.5$)

$$\frac{(A_k^{j+1} - A_k^j) + (A_{k-1}^{j+1} - A_{k-1}^j)}{\Delta t} + \qquad (4.3.2)$$

$$+ \frac{(Q_k^j - Q_{k-1}^j) + (Q_k^{j+1} - Q_{k-1}^{j+1})}{\Delta x} = 0;$$

As Q and A in the points (k-1, j), (k, j) and (k-1, j+1) are supposed to be known, eq. (4.3.2) may be written

$$Q_k^{j+1} + \frac{\Delta x}{\Delta t} \cdot A_k^{j+1} + C_1 = 0; \qquad (4.3.3)$$

where C_1 is a known constant.

If the derivatives in the equation of motion written in the form

$$\frac{\partial Y}{\partial x} - \frac{1}{2g}\frac{\partial V^2}{\partial x} - \frac{1}{g}\frac{\partial V}{\partial t} = S_o - S_f \qquad (4.3.4)$$

are approximated in the same way and if

$$S_{fM} = \frac{1}{4}\left[S_{f_k}^{j+1} + S_{f_{k-1}}^{j} + S_{f_{k-1}}^{j+1} + S_{f_{k-1}}^{j}\right]; \qquad (4.3.5)$$

where S_f is defined by eq. (3.1.3) or by the Manning formula, the equation of motion may be written

$$f(Q_k^{j+1}, A_k^{j+1}) = 0; \qquad (4.3.6)$$

as $V = Q/A$ and Y = unique function of A.

The eqs. (4.3.3) and (4.3.6) form a pair of nonlinear algebraic equations in the unknowns Q_k^{j+1} and A_k^{j+1}, which can be solved by an iterative procedure, for instance the Newton-Raphson method. Thus, with known values of Q and A on line x_{k-1}, those on line x_k can be determined by successive application of the eqs (4.3.3) and (4.3.6). The starting conditions at the upstream boundary are obtained from the initial conditions and by using the backward characteristic equation together with the boundary condition (the inflow hydrograph).

The calculation scheme described above (in the following called the CTH-transport model) implies a more complete box-scheme formulation of Saint-Venant equations than the EPA-model, which neglects the term $\partial V/\partial t$ and which does not use the complete box-scheme for the approximation of the equation of motion. However, there does not seem to be any computational reason not to use the full box-scheme in the CTH-transport model.

The EPA-model was proved to be unconditionally stabel (i.e. for any choice of Δx and Δt) for w_t and w_x both greater than 0.5. A value of 0.55 was chosen since it resulted in the best attentuation of the hydrograph peaks.

It is readely seen that neither the EPA- nor the CTH-transport model consider backwater effects, as the unknowns on line x_k are calculated disregarding the conditions on line x_{k+1}. However, as mentioned earlier, the box-scheme may be used also in implicit schemes [41].

It has to be pointed out that the EPA storm water runoff model, besides the transport model, contains routines accounting for infiltration, overland flow, storage and routing of hydrographs and pollutographs through the receiving waters.

4.4 The kinematic wave approach

The most simplified routing routine is obtained if the routed hydrograph is considered as a kinematic wave. However, it appears from section 3.4 that this is a good approximation only on steep slopes, that is, if secondary slope terms in the equation of motion are small compared to the bottom slope S_o. Although this is certainly not always the case, some authors claime that the kinematic wave provides a good approximation to a wide range of flows.

The kinematic wave is defined by the equation of continuity and the equation of motion in the form, see section 3.4.

$$\begin{cases} \dfrac{\partial Q}{\partial x} + \dfrac{\partial A}{\partial t} = 0 & \text{(4.4.1a)} \\ Q = A\,(8g S_o R/f)^{1/2} = Q(A); & \text{(4.4.1b)} \end{cases}$$

Analyzing this equations by the method of characteristic or following the discussion in section 3.4 we obtain

$$\left.\begin{aligned} \frac{dQ}{dt} &= 0; \\ \frac{dA}{dt} &= 0; \end{aligned}\right\} \quad \text{valid for} \quad \frac{dx}{dt} = c = \frac{dQ}{dA}; \qquad (4.4.2)$$

where c is the kinematic wave velocity. This means that Q and A appear to have constant values by an observer moving with the velocity $dx/dt = c$. Thus, Q and A, and consequently also dQ/dA, have constant values along the characteristic $dx/dt = dQ/dA$.

If the inflow hydrograph at point $x_1 = x$ is $Q = Q(t_1)$ the routed hydrograph at point $x_2 = x + \Delta x$ is given by

$$Q\,(t_1 + \Delta t) = Q(t_1); \qquad (4.4.3)$$

where Δt is obtained by integration of the characteristic.

$$\int_x^{x+\Delta x} dx = \left[\frac{dQ}{dA}\right]_{Q=Q(t_1)} \cdot \int_t^{t+\Delta t} dt;$$

$$(4.4.4)$$

$$\Delta t = \frac{\Delta x}{\left[\dfrac{dQ}{dA}\right]_{Q=Q(t_1)}};$$

As Δt is a function of dQ/dA, the hydrograph is distorted but it maintains its maximum discharge and depth, see fig. 3.7.

The integration performed above, does not give the values of discharge at the same time at point x_2 as at point x_1. However, values for fixed intervals of Δt may be obtained by interpolation between the computed values.

A numerical solution of eq. (4.4.1) may be obtained by application of the finite box-scheme approximation, which gives

$$\frac{(A_k^{j+1} - A_k^j) + (A_{k-1}^{j+1} - A_{k-1}^j)}{\Delta t} + \frac{(Q_k^j - Q_{k-1}^j) + (Q_k^{j+1} - Q_{k-1}^{j+1})}{\Delta x} = 0;$$

$$Q_k^{j+1} = Q\,(A_k^{j+1}); \tag{4.4.5}$$

Also in this case Q and A at the points (k-1, j), (k, j) and (k-1, j+1) are supposed to be known. Q_k^{j+1} and A_k^{j+1} are thus solved by the same procedure as in section 4.3.

Routing routines based on the kinematic wave equations are used in the runoff models described in ref. [6] and [9].

4.5 The Road Research Laboratory (RRL) storage-routing routine

The RRL-method [7, 8] was developed to overcome the drawbacks in rational type methods [43] (peak flow methods), which neglect the reservoir retention in the storm drains.

The RRL-method considers the variation of rainfall intensity with time and calculates the whole outflow hydrograph taking into account only paved surfaces directly connected to the sewer system.

The storage-routing routine used for routing of the inflow hydrograph is as follows:

Let the inflow hydrograph be given by the curve P and the outflow hydrograph by the curve Q in fig. 4.5. If W_n and W_{n-1} are the total storage at times t_n and t_{n-1}, respectively, between the inlet and the outlet sections, we then have with $t_n - t_{n-1} = \Delta t$,

$$W_n - W_{n-1} = \left[(P_n - Q_n) + (P_{n-1} - Q_{n-1})\right] \cdot \Delta t/2$$

or

$$W_n + \frac{Q_n \Delta t}{2} = \frac{\Delta t}{2}\,(P_n + P_{n-1} - Q_{n-1}) + W_{n-1}; \qquad (4.5.1)$$

In eq. (4.5.1) the right hand side is always known from the previous computation and from the inflow hydrograph.

To solve for Q_n and W_n, we need a relation between the storage W and the discharge Q. It is thus assumed in the method, that the relative depth Y/D is the same everywhere in the system and that the discharge-depth relation follows eq. (4.4.1b). For a pipe segment Δx of constant diameter and bottom slope we then have

$$\begin{cases} W_n = A_n \cdot \Delta x \\ Q_n = Q(A_n) \end{cases} \qquad (4.5.2)$$

where A_n is the wet area at the outlet. Both Q_n and W_n can now be found from eqs. (4.5.1) and (4.5.2). This step-by-step solution developes the entire outflow hydrograph.

The original RRL-method considered the whole drainage system in one operation. In a more recent version [44] the storage-routing routine is applied successively to pipe by pipe, starting from the upstream end.

A comparison of the RRL-method with the kinematic wave approach shows clearly the features of the RRL-method. It is readely seen that, using the notations of eq. (4.4.5), eq. (4.5.1) and eq. (4.5.2) take the form

$$\begin{aligned} &\frac{A_k^{j+1} - A_k^j}{\Delta t} + \frac{(Q_k^j - Q_{k-1}^j) + (Q_k^{j+1} - Q_{k-1}^{j+1})}{\Delta x} = 0; \\ &Q_k^{j+1} = Q\,(A_k^{j+1}); \end{aligned} \qquad (4.5.3)$$

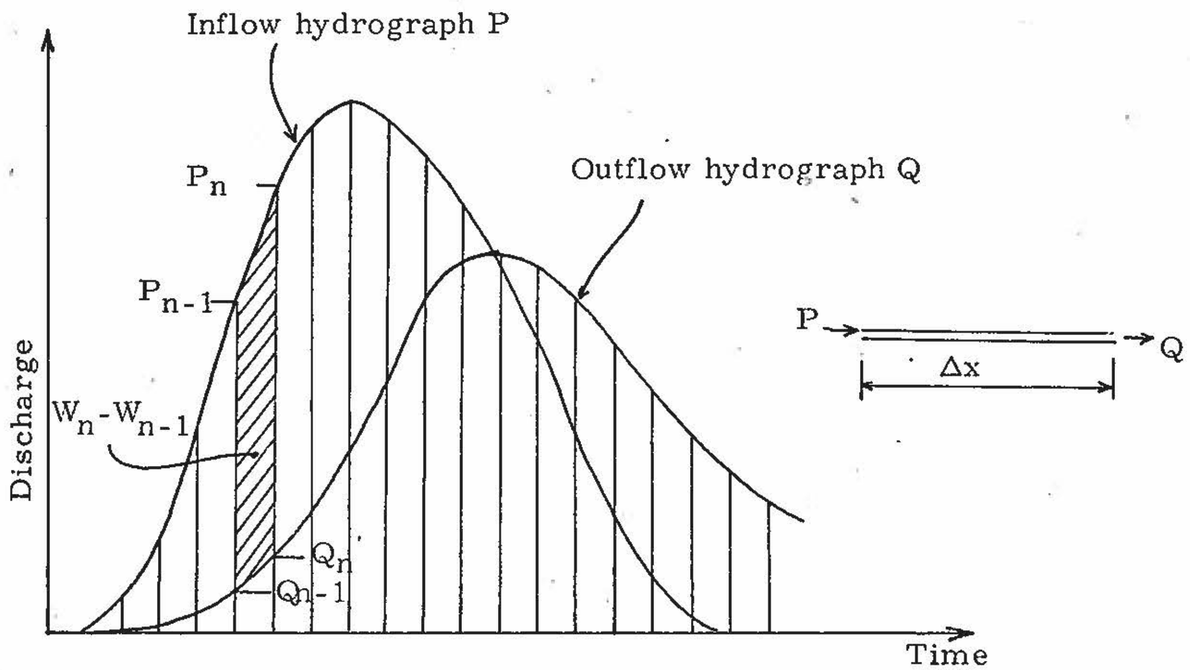

Fig. 4.5 The RRL storage-routing technique.

Outflow and inflow to the pipe element Δx are thus correctly considered in the equation of continuity while the storage volume is determined from the downstream condition A_k^{j+1} and A_k^j, only (the proportional depth approach). The only difference between the RRL storage-routing routine and the kinematic wave is the poor approximation of the storage volume in the RRL-method. It may thus be stated that the RRL-routine is basically a kinematic wave approach.

The RRL-routine leads to subsidence of the flood crest, see fig.4.5. However, this "realistic" behaviour of the routing wave arises from an "unrealistic" approximation of the continuity equation. It will be shown in chapter 5 that the subsidence of the wave depends on the magnitude of the length increment Δx and that the RRL-routine passes into the kinematic wave approach as $\Delta x \rightarrow 0$.

4.6 The NIVA sewer network model

The NIVA network model may be characterized as a modified RRL storage-routing routine. However, it will be shown that the introduced modification implies an impairment of the RRL-method, which itself is relatively weak. Following ref. [2] the NIVA model is as follows:

The inflow hydrograph is routed through each sewer line Δx by a translatation procedure and a storage procedure.

In the translatation procedure each discharge D_n on the inflow hydrograph is translatated the amount of time Δt_n given by

$$\begin{cases} \Delta t_n = \Delta x / (D_n / A_n) \\ D_n = D(A_n) \quad \text{according to eq. (4.4.1b)} \end{cases} \tag{4.6.1}$$

the procedure implying only a distortion of the hydrograph, which maintains its peak discharge and depth. The translatated hydrograph is called P.

In the storage procedure, the translatated hydrograph P is manipulated by the RRL routine, eq. (4.5.1) and the outflow Q is found by the previous described step-by step calculation.

The actual meaning of this two step procedure is that the inflow hydrograph is routed two times through each sewer line, which roughly estimated leads to a doubling of the time of routing of the hydrograph.

Discussions between the author and the NIVA have led to the decision of replacing the actual routing procedure by a routin based on the EPA- or the CTH-transport model.

The NIVA network model is one of the submodels in a complete sewer system model including also treatment plant models and economical models.

5. COMPARATIVE TEST OF METHODS FOR FLOOD ROUTING IN STORM DRAINS

At present the author has only a very limited amount of data available which can be used for comparison of hydrographs predicted by the models described in chapter 4. However, some results reported in ref. [3] can be used as a basis for exemplification of the features of the routing routines.

In ref. [3], the EPA transport model is tested against an "exact" solution. The exact solution was attained numerically by the method of characteristics. The test was performed for a pipe of constant diameter and bottom slope

diameter D	=	1,82 m
bottom slope S_o	=	10^{-3}
full capacity Q_o	=	4.15 m^3/s
length	=	9150 m

The inflow hydrograph consisted of a triangular hydrograph superimposed on a constant base flow, see fig. 5.1.

The results from the EPA-test are presented in fig. 5.2 and 5.3 for different time steps and distance increments. The outflow hydrographs predicted using the EPA-transport model show good agreement with those obtained by the method of characteristics. The characteristics solution was tested against the measured depth hydrographs of ref. [12] and found to be in very good agreement.

The tests indicate the EPA transport model to be an reliable tool for flow routing in pipes in case of no backwater effects.

The proposed CTH-transport model, which is a complete box-scheme formulation of the governing equations, has not yet been tested. However, this model should be at least as good as the EPA-model.

As pointed out in section 4.5, using the RRL-routine, the subsidence of the wave depends on the magnitude of the length increment Δx. This fact is evident from fig. 5.4, which also shows that the RRL-routine passes into the kinematic wave approach as $\Delta x \rightarrow 0$.

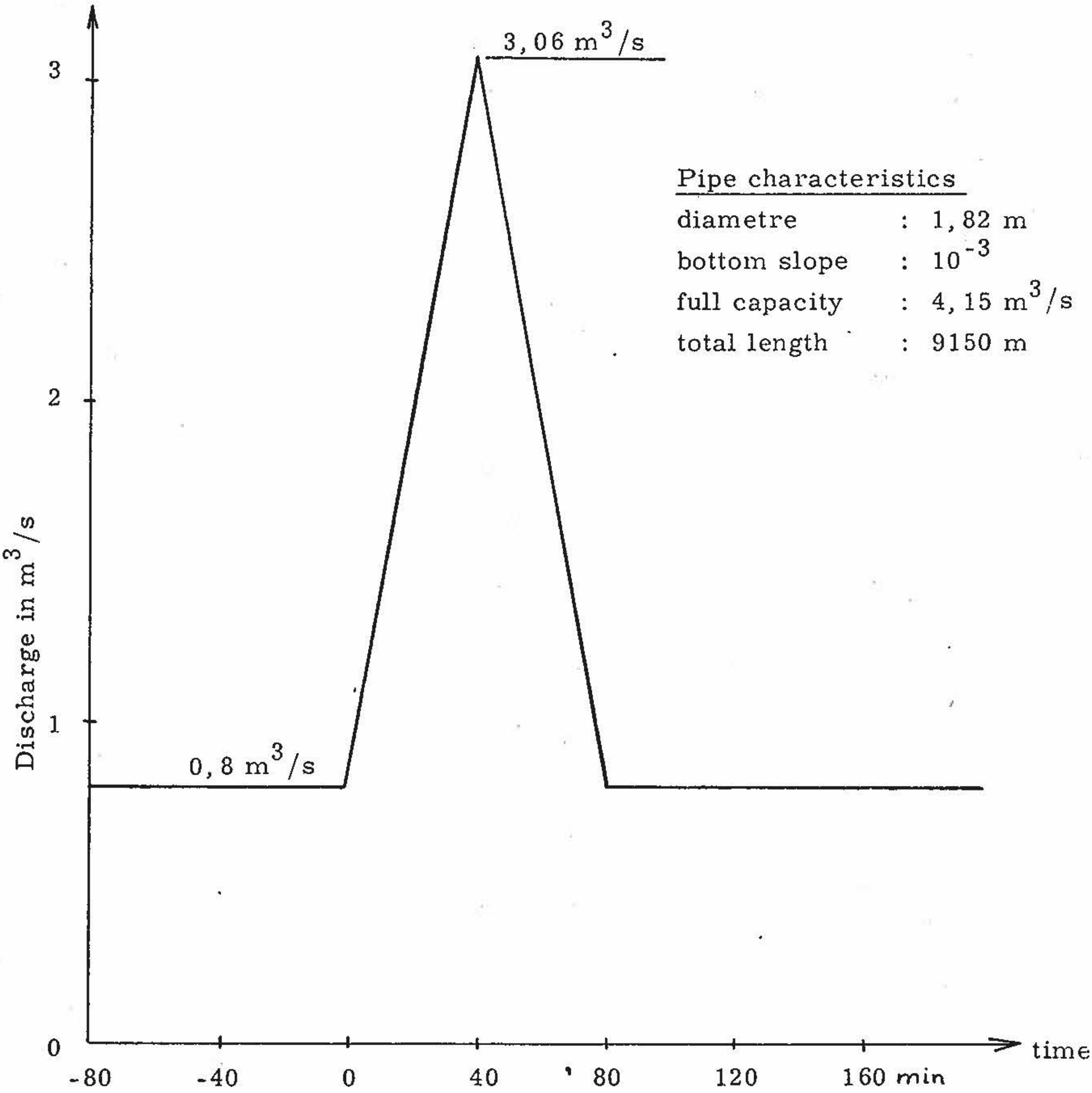

Fig. 5.1 Inflow hydrograph and pipe characteristics for the comparative test.

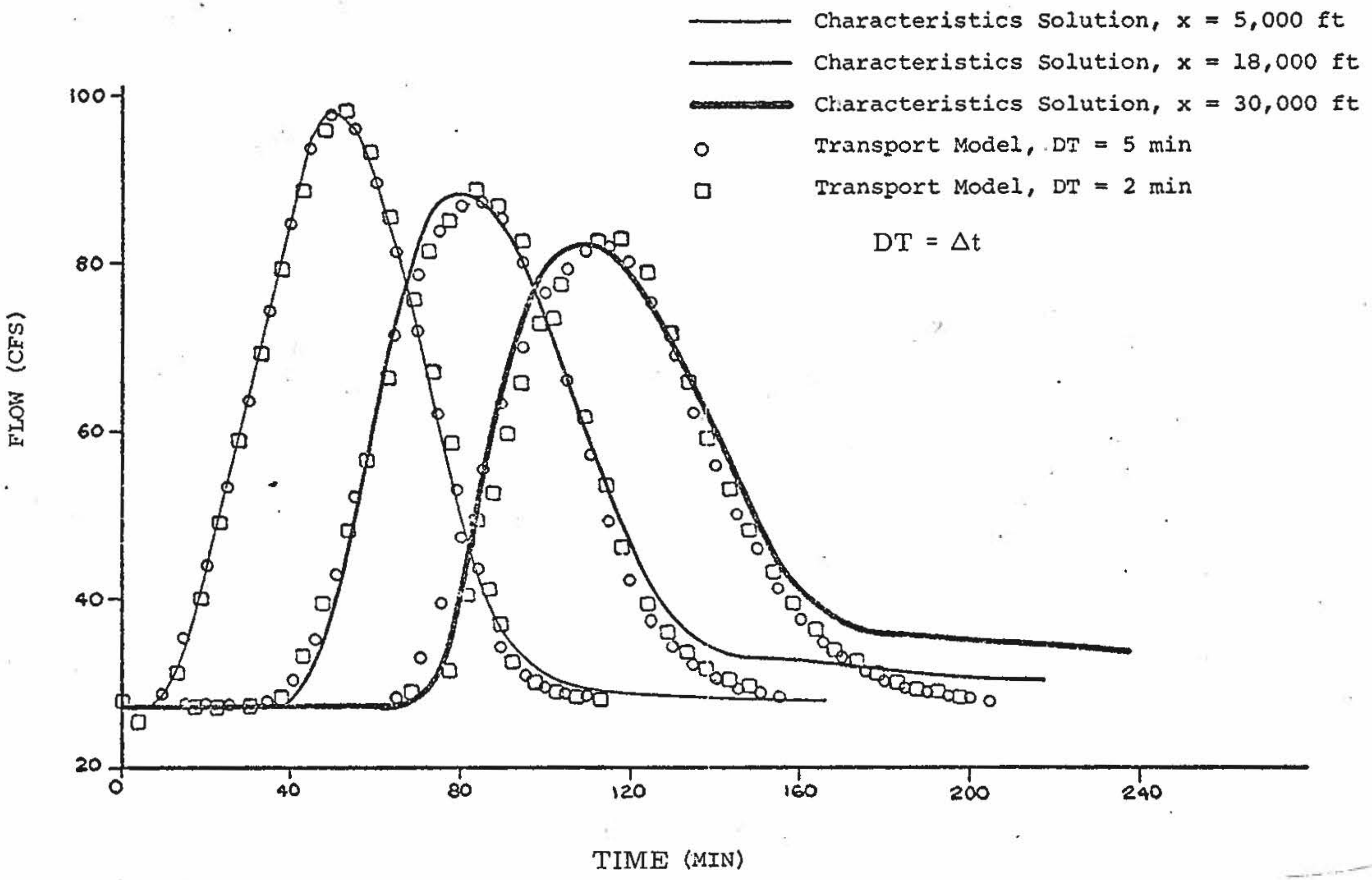

Fig. 5.2 Comparison of EPA transport model and exact solutions for pipeline consisting of 8 conduit lengths. (From ref. [3]).

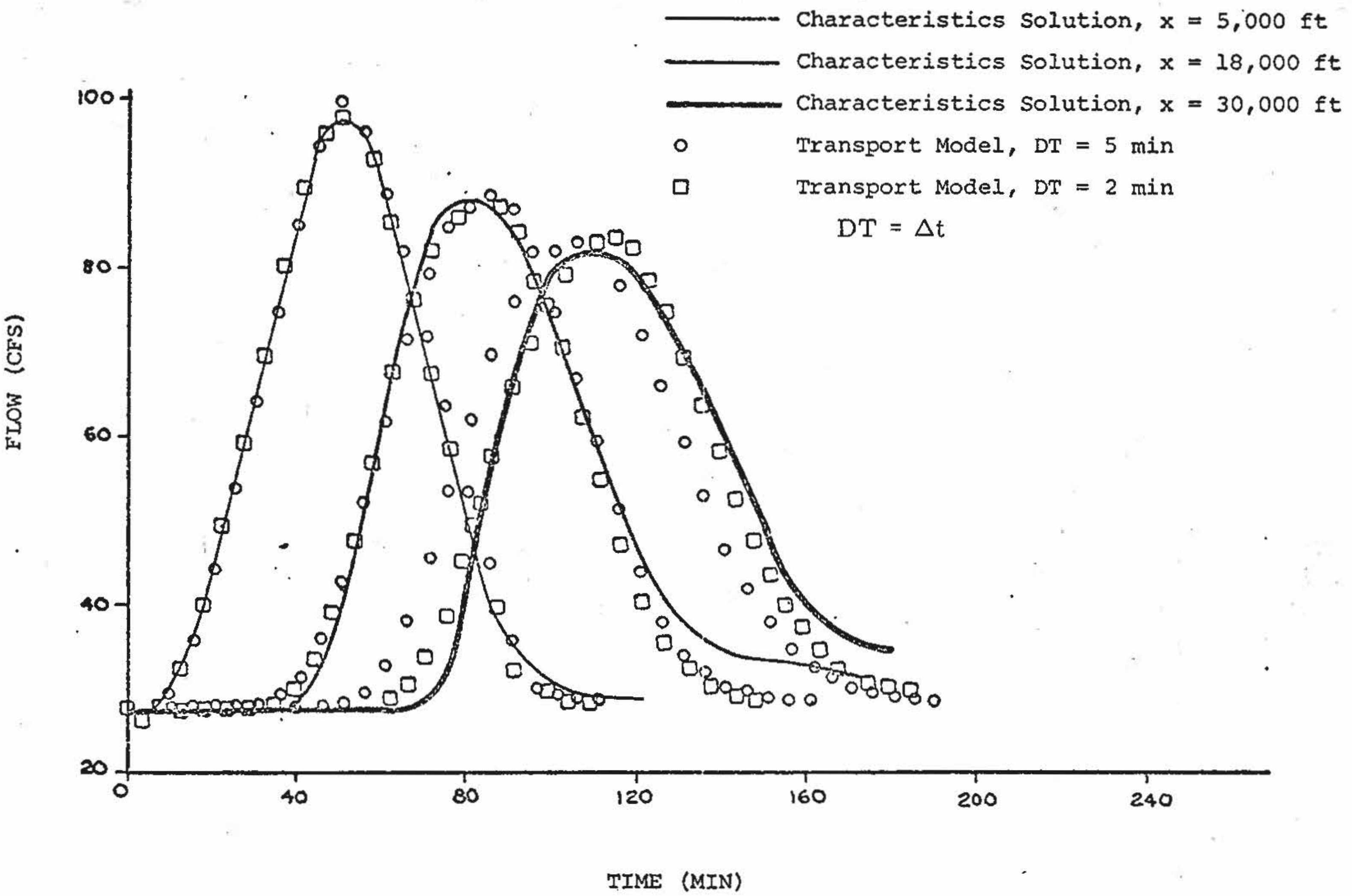

Fig. 5.3 Comparison of EPA transport model and exact solutions for pipeline consisting of 15 conduit lengths. (From ref. [3]).

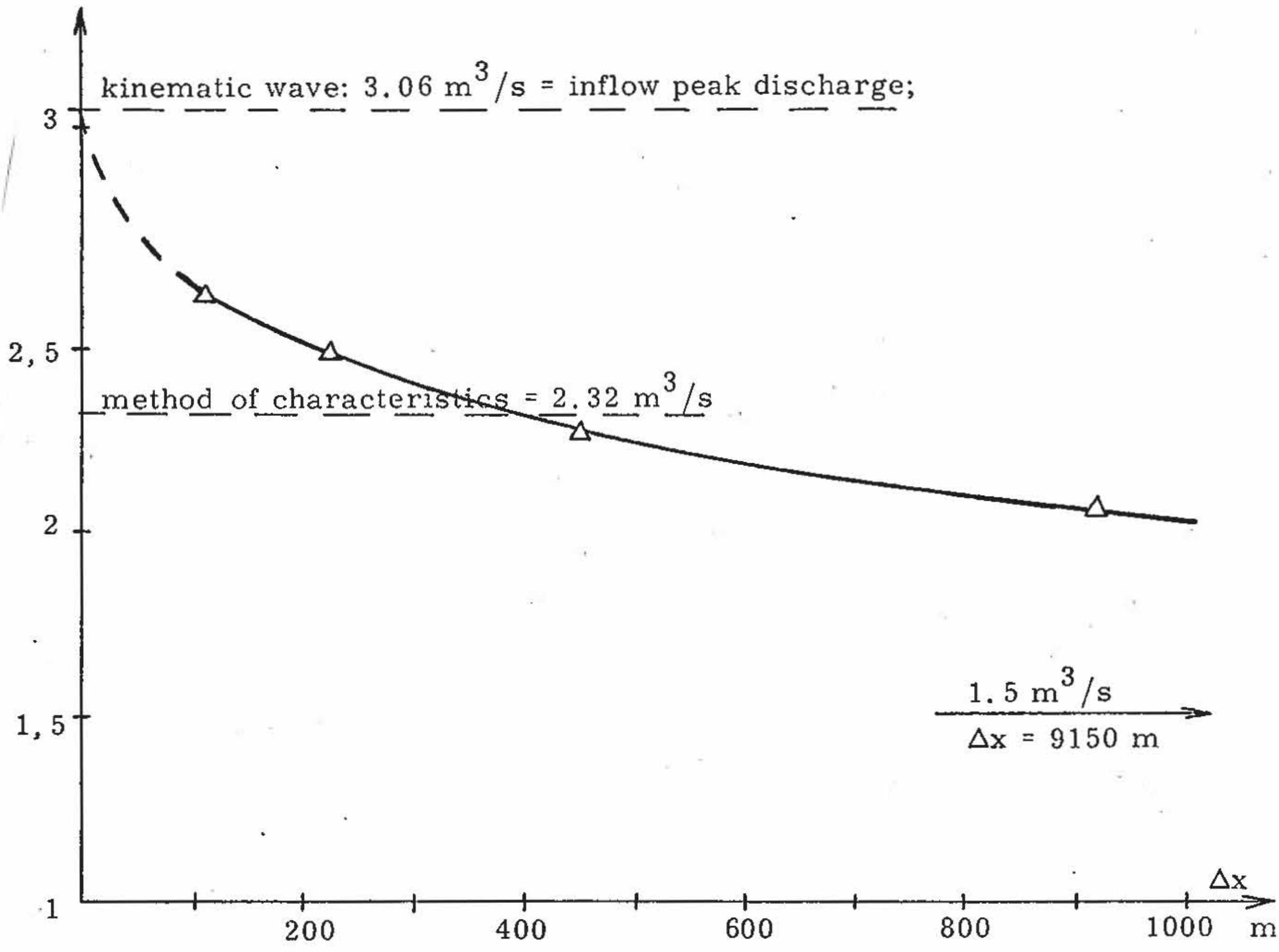

Fig. 5.4 Outflow peak discharge dependence on the length increment Δx used in the RRL storage - routing - routine. Pipe characteristics and inflow hydrograph according to Fig. 5.1.

The effect of the adding of a translatation procedure to the RRL storage-routing routine, as made in the NIVA network model, appears from fig. 5.5. Thus, the time of routing is roughly doubled. It is also shown that the RRL-method may give an approximately correct outflow hydrograph, if Δx is properly chosen. However, as we have no basis for this choice, any agreement is accidental.

Good agreement between the kinematic wave velocity and the actual wave speed is also demonstrated. This agreement is due partly to the small variation of dQ/dA within the actual interval of Q, partly to the fact that the speed of a subsiding wave differs only in second order terms from the kinematic wave speed, see section 3.5.

In order to complete this comparative test we have also included the outflow hydrograph calculated by the routing procedure proposed in ref[46], the University of Cincinnati urban runoff model (UCUR). In this model, the average velocity with which the total inflow volume moves downstream is considered to be the weighted average of all the partial velocities with respect to the corresponding volumes. The inflow hydrograph is thus shifted in time without changing in shape and the hydrograph maintains its peak discharge. The UCUR-method thus corresponds to a "kinematic shock" approach, see section 3.4.

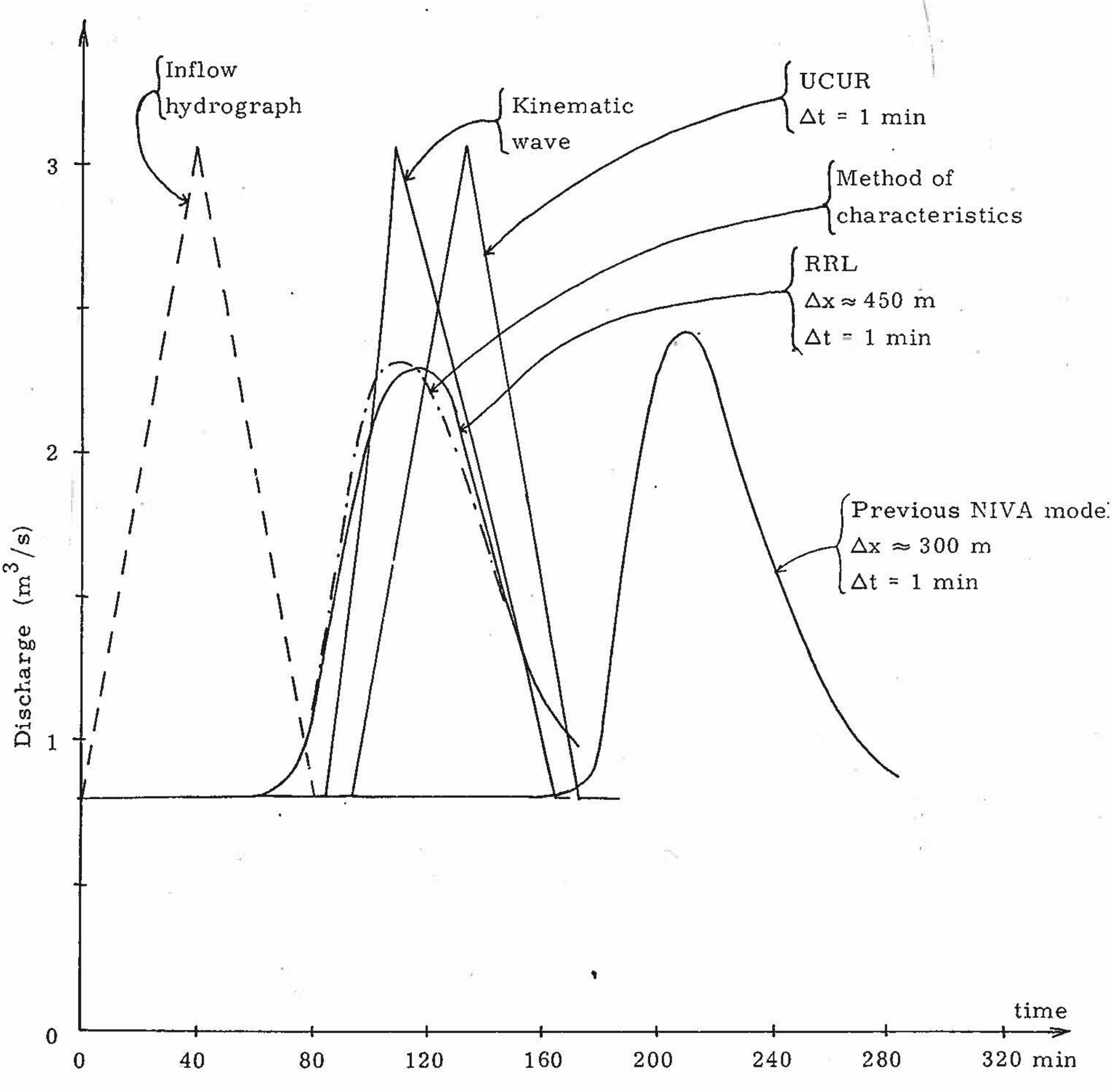

Fig. 5.5 Predicted outflow hydrographs ($x = 9150$ m) by various methods for the condition given in Fig. 5.1.

6. CONCLUSIONS AND RECOMMENDATIONS

Flood routing models applicable to storm drains may be divided in two groups

(a) models which give an adequate simulation of unsteady free surface flow, including simulation of transient backwater conditions

(b) models which give only an approximate simulation of flow conditions

Type (a) models are based on exact solutions of the Saint-Venant equations simultaneously throughout the sewer system. However, the complete boundary conditions, including multijunctions, manholes etc make the programming difficult and the computational costs high. The urban runoff model presented briefly in ref [5] is probably of this type.

In type (b) models, storm water hydrographs are routed independently of downstream conditions. Thus, simulation of transient backwater effects is not possible. These models are less complicated and require a reduced number of geometrical input data. Only conduit lengts, diameters and slopes are required.

Urban runoff models developed in the United States as well as the RRL-model and the NIVA-model use routing submodels based on type (b) flow models. The authors of these methods claim that, considering the great uncertainties in inputdata (precipitation, infiltration rates, surface storage and surface runoff etc), the accuracy of their models are sufficient for practical purposes and that computational costs should be too high for a type (a) model. The most accurate existing type (b) model is the so called EPA-transport model.

Considering the remarques given above, the author suggests the following planning of the continued studies:

1. Development of a complete routing routine based on the EPA- or the CTH-transport models. This work has in fact already started in cooperation with the Norwegian Institute for Water Research (NIVA). This routing routine will thus replace the present routine in the complete sewer network model developed by NIVA. The model will give an approximate picture of backwater effects and overflow conditions.

2. Development of a preliminary routing routine based on a type (a) model in order to investigate programming difficulties and computational costs and for studies of the degree of approximation of the type (b) model. For the development of the type (a) model, which most likely will be of the implicit - non linear type, use of the experience obtained within the work with the model presented in ref [47], will be made. The reason for using a nonlinear system is the problems concerning linearization of complexe boundary conditions.

3. Test of mathematical models in a hydraulic laboratory model. The hydraulic model should also render possible studies of junction problems.

7. REFERENCES

1 Lindholm, O: Systemanalys av avlopsanlegg. - (Vatten vol 29 (1973) No 2 and Norsk Institutt for Vannforsknings Arsbok 1972. Oslo, 1973).

2 Lindholm, O: Modelling of sewerage systems. - (Symposium on the Use of Mathematical Models in Water Pollution Control. University of Newcastle upon Tyne, 10-14 September 1973).

3 Lager, J A, Pyatt, E E and Shubinski, R P: Storm Water Management Model Volume I. Final Report. - (Environmental Protection Agency. (EPA). Water Quality Office. Water Pollution Control Research Series. Report No 11024 DOC 07/71. Washington, July 1971).

4 Ritter, F G and Warg, G: Upgrading city sewer installations - (Engineering Digest, April 1971).

5 Warg, G: Die Ganglinien - Volumen - Methode fur elektronische Kanalnetzberechnungen. - (Wasser und Boden. Heft 8/1968).

6 Schaake, J C: Deterministic Urban Runoff Model (Treatise on Urban Water Systems edited by Albertson, Tucker and Taylor. Chapter VIC. Colorado State University, Fort Collins, Colorade July, 1971).

7 Watkins, L H: The Design of Urban Sewers Systems. (Road Research Technical Papers No 55. Dept. of Scientific and Industrial Research, London 1962).

8 Terstriep, J B and Stall, J B: Urban Runoff by the Road Research Laboratory Method. (ASCE Journal of Hydraulics Division, No 95, November 1969).

9 Amorocho, J et al.: Simulation of Runoff from Arid and Semiarid Climate Watersheds. Volume I. (Under preparation) (Department of Water Science and Engineering. University of California, Davis).

10 Papadakis, C and Preul, HC: University of Cincinnati Urban Runoff Model. (ASCE Journal of Hydraulics Division, Vol 98, HY 10, October 1972).

11 Stall, J B and Terstriep, M L: Storm Sewer Design - An Evaluation of the RRL - Method – (U.S. Environmental Protection Agency, Washington, EPA - R2-72-068, October 1972).

12 Yevjevich, V and Barnes, A H: Flood Routing through Storm Drains. Part I. Solution of Problems of Unsteady Flow in Storm Drains - (Hydrology Paper No 43 Colorado State University, Fort Collins, Colorado, November 1970).

13 Brutsaert, W: De Saint-Venant equations experimentally verified (ASCE, Journal of Hydraulics Division, HY9, September, 1971).

14 Cunge, J A and Wegner, M: Intégration Numéerique des Equations d´Ecoulement de Barré de Saint-Venant par un Schéma Implicite de Différences Finies (La Houille Blanche, No 1, 1964).

15 Ellis, J:Unsteady Flow in Channel of Variable Cross Section (ASCE, Journal Of Hydraulics Division, No HY10, October, 1970).

16 Eagleson, P S: Unit Hydrograph Characteristics for Sewered Areas (ASCE, Journal of Hydraulics Division, Vol. 88, No HY2, March, 1962).

17 Daily, J W and Harleman, D R F: Fluid Dynamics. - (Addison-Wesley Publ. Comp. 1966).

18 Whitaker, S: Introduction to Fluid Mechanics. - (Prentice-Hall, Inc. Englewood Cliffs. N.J. 1968).

19 Rouse, H: Advanced Mechanics of Fluids - (John Wiley and Sons, Inc. New York. 1959).

20 Hildebrand, F B: Advanced Calculus for Applications. - (Prentice-Hall, Inc. Eaglewood Cliffs. N.J. 1962).

21 Aris, R: Vectors, Tensors and the Basic Equations of Fluid Mechanics. - (Prentice-Hall Inc. Eaglewood Cliffs. N.J. 1962).

22 Strelkoff, T: The One-Dimensional Equations of Open Channel Flow. - (Journal of the Hydraulics Division, ASCE, Vol. 95, No HY3, May, 1969).

23 Rouse, H, Siao, T T and Nagaratnam, S: Turbulence Characteristics of the Hydraulic Jump. - (Transactions, ASCE, Vol 124, 1959).

24 Hubbard, P G: Discussion of "Turbulence Characteristics of the Hydraulics Jump", by Rouse, Siao and Nagaratnam.

25 Hinze, J O: Turbulence - (Mc Graw-Hill Book Comp. New York 1959).

26 Yevjevich, V and Barnes, A H: Flood Routing through Storm Drains. Part I. Solution of Problems of Unsteady Free Surface Flow in Storm Drains (Hydrology Paper No 43, Colorado State University. Fort Collins, November 1970).

27 Henderson, F M: Open Channel Flow. (The Macmillan Company, New York, 1966).

28 Hildebrand, F B: Advanced Calculus for Applications (Prentice-Hall, Inc. Englewood Cliffs, New Jersey 1962).

29 Stoker, J J: Water Waves (John Wiley and Sons, Inc., New York, 1957).

30 Lighthill, M I and Whitham, G B: On Kinematic Waves. I. Flood Movement in Long Rivers. (Proceedings of the Royal Society of London. Vol. 229, no 1178. May 1955).

31 Eagleson, P S: Dynamic Hydrology (Mc Graw-Hill Book Company, Inc. New York 1970).

32 Henderson, F M: Flood Waves in Prismatic Channels. (Proc. Amer. Soc. Civil Engrs. Journal of the Hydraulics Division. Vol. 89. No. HY4, July 1963).

33 Hayami, S: On the Propagation of Flood Waves (Disaster Prevention Research Institute. Kyoto University. Bulletin No 1. December, 1951).

34 Yevjevich, V and Barnes, A H: Flood Routing through Storm Drains. Part IV. Numerical Computer Methods of Solution - (Hydrology Papers No 46, Colorado State University, Fort Collins, Colorado, November, 1972).

35 Mozayeny, B and Song, C S: Propagation of Flood Waves in Open Channels - (ASCE, Journal of Hydraulics Division. Vol 95, No HY3. May 1969).

36 Strellkoff, T: Numerical Solution of Saint-Venants equations - (ASCE Journal of Hydraulics Division, Vol. 96, No. HY1, January 1970).

37 O´Brien, G G, Hyman, M A and Kaplan, S: A Study of the Numerical Solution of Partial Differential Equations - (Journal of Mathematics and Physics. Vol. 29, 1950).

38 Smith, G D: Numerical Solution of Partial Differential Equations - (Oxford University Press, London 1965).

39 Vreugdenhill, G B: The accuracy of the method of computation for unsteady flow in open-channel networks. - (Delft Hydr. Lab. Research report S89-I, January 1968).

40 Cunge, J A and Wegner, M: Intégration Numerique des Equations d´Ecoulement de Barré de Saint-Venant par un Schéma Implicite de Differences Finies - (La Houille Blanche, No 1, 1964).

41 Amein, M and Fang, C S: Implicit Flood Routing in Natural Channels - (ASCE. Journal of Hydraulics Division, Vol 96, No HY12. December 1970).

42 Stapel, D R A and De Vries, M: Experience with the Mathematical Model of the Hydraulic Network of Rijnland Water Board - (Delft Hydraulics Laboratory. Publ. No 74, October 1970).

43 Lindh, G and de Maré, L: Calculation of urban storm water runoff. A literature review (in Swedish) - (Division of Hydraulics, Institute of Technology/University of Lund. Bulletin Serie A Nr 9, 1972).

44 Watkins, L H: Discussion of ref. 11, Urban Runoff by Road Research Laboratory Method - (ASCE, Journal of Hydraulic Division, Vol 96, No HY7, July 1970).

45 Meijer, J G P, Vreugdenhil, C B and De Vries, M: A method of computation for non-stationary flow in open-channel networks - Hydraulics Laboratory Delft, Publ. No. 34, September 1965.

46 Division of Water Resources Department of Civil Engineering, Univ. of Cincinnati: Urban Runoff Characteristics. - (Interim Report for the Environmental Protection Agency, Water Quality Office. Water Pollution Control Research Series. Report No 11024 DQU 10/70. Washington, October, 1970).

47 Cederwall, K.: Flow models for pipe and tunnel systems (in Swedish) Chalmers University of Technology, Division of Hydraulics, Publ. No 67, Gothenburg 1972).

48 Hansen, J.A.: Numerical analysis of unsteady open channel flow - (Hydraulic Laboratory, Technical University of Denmark. Bull. No. 10, April 1966).

Chalmers Tekniska Högskola

GEOHYDROLOGISKA FORSKNINGSGRUPPEN

Institutionerna för
Geologi
Geoteknik med grundläggning
Vattenbyggnad
Vattenförsörjnings- och avloppsteknik

Meddelande:

nr 1	Urbaniseringsprocessens inverkan på ytvatten-avrinning och grundvattenbildning. Lägesrapporter (1972-07-01 - 1973-03-01). 1973.
nr 2	Leif Carlsson: Grundvattenavsänkning Del 1. Evaluering av akvifärers geohydrologiska data med hjälp av provpumpningsdata. 1973.
nr 3	Leif Carlsson: Grundvattenavsänkning Del 2. Evaluering av lågpermeabla lagers hydrauliska diffusivitet med hjälp av provpumpningsdata. 1973.
nr 4	Viktor Arnell: Nederbördsmätare. En sammanställning av några olika mätartyper. 1973.
nr 5	Viktor Arnell: Dimensioneringsregn för projektering av dagvattenledningar i Göteborg. 1974
nr 6	Urbaniseringsprocessens inverkan på ytvatten-avrinning och grundvattenbildning. Lägesrapporter (1973-03-01 – 1974-02-01). Göteborg 1974.
nr 7	Olov Holmstrand, Per O Wedel: Ingenjörsgeologiska kartor– Litteraturstudier. 1974.